

# Resonant production of heavy particles during inflation and its gravitational wave signature

Qi Chen<sup>a\*</sup> and Yuan Yin<sup>b†</sup>

<sup>a</sup> *Kavli Institute for Theoretical Sciences, University of Chinese Academy of Sciences, Beijing 100190, China*

<sup>b</sup> *School of Physics, Korea Institute for Advanced Study, Seoul 02455, Korea*

## Abstract

We show that a quadratic  $U(1)$ -breaking term, together with an effective chemical potential induced by a dimension-five derivative coupling between the inflaton and the  $U(1)$  current, can drive efficient particle production during inflation even when the  $U(1)$  field is heavier than the Hubble scale. Notably, the chemical potential enables efficient production even when the  $U(1)$ -breaking mass is smaller than the effective diagonal mass. We compute the gravitational-wave signal generated by this mechanism during inflation, derive the primordial tensor spectrum, and map it to the present-day energy density  $\Omega_{\text{GW}}(f)$ . Assuming the  $U(1)$  field constitutes the dominant component of dark matter, this mapping fixes the characteristic frequency, which we compare with projected sensitivity curves of ongoing and proposed gravitational wave observatories. Finally, we argue that the same dynamics are accompanied by a cosmological collider signal, providing an independent cross-validation of the framework.

---

\*Email: [chenqi25@ucas.ac.cn](mailto:chenqi25@ucas.ac.cn)

†Email: [yinyuan@kias.re.kr](mailto:yinyuan@kias.re.kr)

# Contents

<b>1</b>	<b>Introduction</b>	<b>3</b>
<b>2</b>	<b>The model</b>	<b>4</b>
<b>3</b>	<b>Particle production and the constraints</b>	<b>6</b>
3.1	Constraints on the parameters . . . . .	9
<b>4</b>	<b>The gravitational wave from the particle production</b>	<b>9</b>
4.1	The gravitational wave power spectrum . . . . .	11
4.2	From primordial power spectrum to the observable . . . . .	13
4.3	Frequency mapping and the numerical results . . . . .	15
<b>5</b>	<b>The cosmological collider signal</b>	<b>17</b>
<b>6</b>	<b>Conclusion and discussions</b>	<b>18</b>
<b>A</b>	<b>Evolution of the Bogoliubov coefficients</b>	<b>20</b>
<b>B</b>	<b>The stationary phase approximation</b>	<b>22</b>

# 1 Introduction

Inflation is the leading paradigm for the early Universe: it resolves several long-standing puzzles, most notably the horizon problem, and provides a mechanism for generating the primordial perturbations that seed large-scale structure [1–4]. It has also been suggested that the matter–antimatter asymmetry was produced during this epoch [5–16]. Realizing such an asymmetry requires that baryon number not be an exact quantum number when the asymmetry is generated. In broad terms, this points to early-Universe dynamics described by a  $U(1)$ -violating theory. A minimal realization is a quadratic  $U(1)$ -breaking term active during inflation.

A central aim of this work is to assess the phenomenological consequences of a quadratic  $U(1)$ -breaking operator during inflation. Prior studies [17–19] indicate that explicit breaking renders physical the chemical potential induced by a dimension-five EFT interaction, which otherwise removable by a time-dependent field redefinition, thereby leading to characteristic cosmological-collider signatures. However, the detailed particle-production dynamics sourced by this  $U(1)$ -breaking term have not been analyzed systematically.

Particle production during inflation is, in its own right, a natural mechanism for generating heavy dark matter, given that the Hubble scale can be as high as  $10^{14}$  GeV. Nevertheless, superheavy candidates, such as right-handed neutrinos near their upper mass bound or Wimpzillas [20], may have masses exceeding the inflationary Hubble parameter. For such heavy particles, inflationary production suffers the familiar Boltzmann suppression  $e^{-\pi m/H}$ . Consequently, purely inflationary production is typically insufficient, motivating additional mechanisms. Previous proposals include first-order phase transitions during inflation [21], sharp transitions between the inflationary and radiation-dominated epochs [22, 23], axion inflation [24], and scenarios involving inflaton oscillations [25–28]. One can refer to [29] for a comprehensive review.

In this work we demonstrate that an explicit  $U(1)$ -breaking term,  $\chi^2 + \chi^{*2}$ , together with the minimal coupling of the inflaton to the  $U(1)$  current,  $\partial_\mu \phi \mathcal{J}^\mu$ , the very coupling previously explored in the cosmological collider context, suffices to produce such superheavy dark matter efficiently. Because the resulting production is non-thermal, it can evade the exponential suppression associated with large masses or large momenta. This mechanism thus offers a simple and compelling cosmic origin for superheavy dark matter.

A further, inescapable implication of efficient particle production is the generation of a primordial gravitational-wave (GW) signal. In quantum field theory, particles correspond to excitations of the underlying field; large occupation numbers therefore imply substantial field fluctuations and a correspondingly sizable stress–energy tensor. The resulting anisotropic stress acts as a source for tensor perturbations, yielding a stochastic GW background [30].

A broad network of experiments probes such a background across many decades in frequency. Ground-based interferometers (LIGO, Virgo, KAGRA) are sensitive in the  $10\text{ Hz} \sim \text{kHz}$  band [31], while space-based missions (e.g., LISA [32], TianQin [33], Taiji [34]) target the  $\sim 10^{-4}\text{--}10^{-1}\text{ Hz}$  window. Pulsar-timing arrays (including the SKA era) probe  $\sim \text{nHz}$  scales [35–42], and forthcoming CMB Stage-4 measurements [43] will sharpen constraints near  $\sim 10^{-17}\text{Hz}$  via B-mode polarization. By contrast, truly high-frequency GWs with  $f \gtrsim \text{MHz}$  are notoriously difficult to detect: the required detector baselines become small, signal power falls rapidly with size, and instrumental noise does not scale down comparatively, which is an obstacle that has long plagued

attempts to observe GWs from preheating.

In the mechanism proposed here, however, the GWs are sourced during inflation. Consequently, inflation subsequently redshifts these tensor modes to lower present-day frequencies. Depending on when the source is active and on the post-inflationary thermal history, the spectral peak can naturally fall within the kHz, mHz, or nHz bands, placing the signal squarely within the reach of the detectors listed above. Moreover, because the same couplings also imprint distinctive cosmological collider signatures, this framework affords a powerful cross-validation strategy: correlated non-Gaussian features and a stochastic GW background would jointly test the model and help disentangle it from purely post-inflationary production scenarios.

The remainder of this paper is organized as follows. Section 2 introduces the model, presenting the Lagrangian, including the explicit  $U(1)$ -breaking operator and the inflaton–current coupling, and defines a rotated field basis that streamlines the subsequent analysis and fixes our notation. Section 3 analyzes particle production by solving for the Bogoliubov coefficients in the time-dependent background and assign the viable parameter space by imposing the requirement that the dark sector is not overproduced. Section 4 computes the primordial spectrum of the sourced stochastic gravitational wave background and maps it to the present-day spectral energy density  $\Omega_{\text{GW}}(f)$ , enabling direct comparison with the sensitivities of current and forthcoming probes across the kHz, mHz, and nHz bands. We also comment on correlated cosmological collider signatures in Section 5. The Appendix collects technical details, including the derivation of the Bogoliubov system and the stationary-phase approximation employed in our semi-analytic and numerical evaluation of the GW power spectrum.

## 2 The model

During inflation, heavy spectator fields are generically produced only at a Boltzmann-suppressed rate, proportion to  $e^{-2\pi m/H}$ , so purely gravitational production is too feeble to source observable primordial GWs. A controlled way to lift this suppression is to endow the spectator with a time-dependent background that drives non-adiabatic evolution. For fields with non-zero spin, a CP-odd dim-5 operator generates a chemical potential that helicity-selects the amplified modes [44–47]. For a scalar spectator, a chemical potential by itself does not provide helical amplification; however, when combined with a  $U(1)$ -breaking mass term it induces a coherent mixing between particle and antiparticle modes, opening tachyonic/resonant windows and enabling large production.

We adopt the  $(- +++)$  signature and work with a complex scalar  $\chi$  charged under a global  $U(1)$ . The inflaton  $\phi$  slowly rolls,  $\partial_\mu\phi = (\dot{\phi}_0, \mathbf{0})$ , and generates a chemical potential  $\mu \equiv \dot{\phi}_0/\Lambda$  through a dimension-5 derivative coupling. A minimal covariant Lagrangian is

$$\sqrt{-g}\mathcal{L} = \partial_\mu\chi\partial^\mu\chi^* + m^2\chi\chi^* + i\frac{\partial_\mu\phi}{\Lambda}(\chi\partial^\mu\chi^* - \chi^*\partial^\mu\chi) + \frac{A^2}{2}(\chi^2 + \chi^{*2}). \quad (1)$$

The last term breaks  $U(1)$  and will be the driver of particle–antiparticle mixing. CMB bounds on the slow-roll parameter imply  $\dot{\phi}_0 \simeq \sqrt{2\epsilon}HM_{\text{Pl}}$ , so validity of the effective theory requires  $\Lambda \gg H$  (we will later take  $\Lambda \gtrsim 60H$  as a conservative sufficient condition).

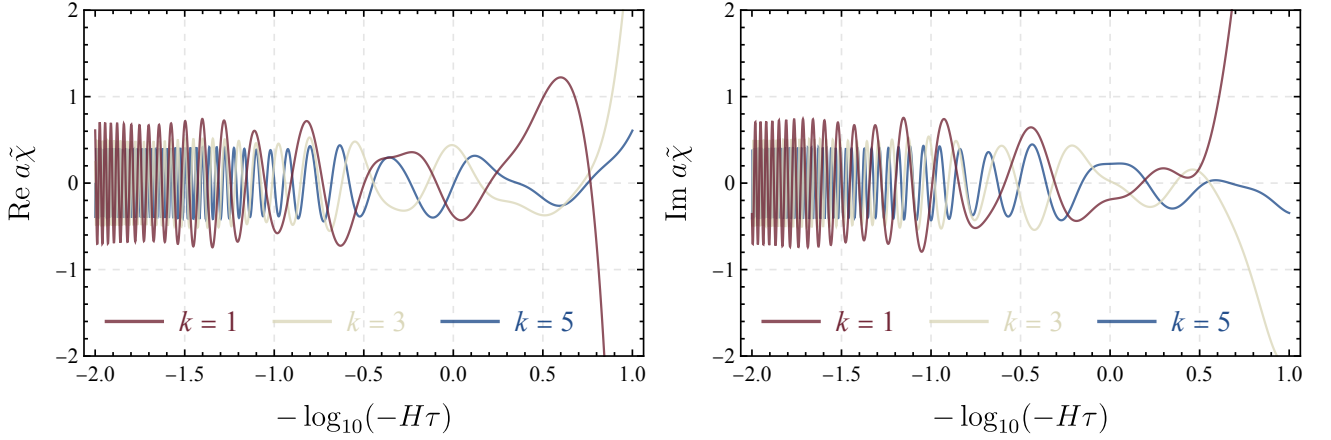


Figure 1: The evolution of the real and imaginary part of the mode function with different momentum.

In a spatially flat FRW background,  $ds^2 = -dt^2 + a^2(t) d\mathbf{x}^2$ , the Lagrangian becomes

$$\sqrt{-g} \mathcal{L} = a^3 |\dot{\chi}|^2 - a |\partial_i \chi|^2 + i a^3 \mu (\chi \dot{\chi}^* - \chi^* \dot{\chi}) - a^3 m^2 |\chi|^2 + a^3 \frac{A^2}{2} (\chi^2 + \chi^{*2}). \quad (2)$$

A time-dependent  $U(1)$  rotation  $\chi = e^{-i\phi_0/\Lambda} \tilde{\chi}$  removes the chemical term and shifts the mass, while the  $U(1)$ -breaking picks up an oscillatory phase. One finds

$$\sqrt{-g} \mathcal{L} = a^3 [ |\dot{\tilde{\chi}}|^2 - (m^2 + \mu^2) |\tilde{\chi}|^2 ] - a \partial_i \tilde{\chi}^* \partial_i \tilde{\chi} + a^3 \frac{A^2}{2} (e^{-2i\mu t} \tilde{\chi}^2 + e^{+2i\mu t} \tilde{\chi}^{*2}). \quad (3)$$

Note that under this base, the  $U(1)$ -breaking term obtain a rotating phase with frequency of  $2\mu$ . Switching to conformal time  $d\tau = dt/a$  and Fourier modes  $\tilde{\chi}(\mathbf{k}, \tau)$ , the Euler–Lagrange equations read

$$\tilde{\chi}'' - \frac{2}{\tau} \tilde{\chi}' + \left[ k^2 + \frac{m^2 + \mu^2}{H^2 \tau^2} \right] \tilde{\chi} + \frac{A^2}{H^2 \tau^2} (-H\tau)^{-\frac{2i\mu}{H}} \tilde{\chi}^* = 0, \quad (4)$$

$$\tilde{\chi}^{*''} - \frac{2}{\tau} \tilde{\chi}^{*''} + \left[ k^2 + \frac{m^2 + \mu^2}{H^2 \tau^2} \right] \tilde{\chi}^* + \frac{A^2}{H^2 \tau^2} (-H\tau)^{\frac{2i\mu}{H}} \tilde{\chi} = 0, \quad (5)$$

where during quasi-de Sitter  $a(\tau) = -1/(H\tau)$  and  $\tau < 0$  while the source is active. The factors  $(-H\tau)^{\pm 2i\mu/H}$  follow from  $e^{\pm 2i\mu t} = (-H\tau)^{\mp 2i\mu/H}$ . The equations explicitly exhibit the mass shift  $m^2 \rightarrow m^2 + \mu^2$ , the Hubble friction term  $-2\tilde{\chi}'/\tau$ , and the oscillatory mixing  $\propto A^2 \tilde{\chi}^*$  that drives particle production. In Figure 1, we solve the equation of motion numerically.

**The switch sector** In our setup the  $U(1)$ -breaking operator is active only for a finite interval  $(\tau_i, \tau_*)$  during the inflation. A natural realization is to take its coefficient  $A$  as  $A \equiv \tilde{A}, v_\sigma$ , where  $v_\sigma$  is the vacuum expectation value of a field  $\sigma$  that undergoes SSB during inflation. To keep the physics transparent, we treat  $v_\sigma$  as piecewise constant, switching on and off sharply. A concrete implementation uses a hybrid trigger in which the  $\sigma$  vev is induced and later removed by a

waterfall field  $X$ :

$$V(\phi, X, \sigma) = V_{\text{inf}}(\phi) + \frac{\lambda_\sigma}{4}(\sigma^2 - v^2)^2 + \frac{1}{2}(M^2 - c^2\phi^2)X^2 + \frac{\lambda_X}{4}X^4 + \frac{1}{2}g^2X^2\sigma^2, \quad (6)$$

For  $|\phi| < M/c$  the minimum has  $X = 0$ , so  $\sigma$  sits in the broken phase with time-independent  $\langle \sigma \rangle = \pm v$ ; for  $|\phi| > M/c$ ,  $X$  acquires an inflaton-modulated vev and, via the portal term, restores the symmetry, driving  $\langle \sigma \rangle \rightarrow 0$ . Our conclusions do not hinge on the microphysics of this trigger sector—the potential above is simply one economical example among many viable realizations of finite-time  $U(1)$  breaking during inflation.

**EFT and consistency.** Throughout we keep  $\Lambda \gg H$  and  $\mu \ll \Lambda$  so that higher-dimensional operators remain negligible. Backreaction is controlled by the fractional energy in produced quanta  $f_\chi \equiv \rho_\chi/(3M_{\text{Pl}}^2 H^2) \ll 1$ , which we will discuss in detail in Sec 3.1;

**Remark on the base choice** A remark is necessary regarding the two bases,  $\chi$  and  $\tilde{\chi}$ , employed in our setup. The free part's Lagrangian (1) is equivalent to that of two real scalar fields,  $\chi = (\chi_+ + i\chi_-)/\sqrt{2}$ , corresponding to the real and imaginary parts of  $\chi$ . In this picture, the mass of  $\chi_+$  is increased by the  $A^2$  term, while the mass of  $\chi_-$  is suppressed by it. Consequently, for large  $A$  values that exceed the diagonal mass  $m$ , the  $\chi_-$  field becomes tachyonic. As a result, a Hamiltonian that is not bounded from below cannot be constructed in the  $\chi$ -basis. Therefore, to obtain a unified description valid for all values of  $A$ , we adopt the  $\tilde{\chi}$ -basis. In this framework, the term proportional to  $A^2$  is regarded as an oscillating pump that drives the system. Hereafter,  $\chi$  will be used as a shorthand notation for  $\tilde{\chi}$  for simplicity, unless explicitly stated otherwise.

### 3 Particle production and the constraints

Purely gravitational production of a heavy spectator during inflation is exponentially suppressed, and by itself cannot source an observable stochastic GW background. In our setup a dimension-5 derivative coupling endows the complex scalar  $\chi$  with an effective chemical potential  $\mu \equiv \dot{\phi}_0/\Lambda$ . A  $U(1)$ -breaking mass term, then mixes particle and antiparticle modes. After removing the chemical term by a time-dependent  $U(1)$  rotation, the  $U(1)$ -breaking operator acquires an oscillatory phase  $e^{\pm 2i\mu t}$ . This acts as a coherent “pump” that periodically violates adiabaticity and drives pair production of  $\chi$  quanta. The key advantage is control: the chemical potential shifts the diagonal mass  $m^2 \rightarrow m^2 + \mu^2$  preventing a broad, catastrophic tachyonic instability, while the time-dependent off-diagonal mixing still enables efficient, localized resonant bursts. This mechanism naturally imprints a logarithmically oscillatory pattern in time (and hence in wavenumber).

Passing to conformal time and defining the canonical field

$$u(\tau, \mathbf{x}) \equiv a(\tau)\chi(\tau, \mathbf{x}), \quad u_{\mathbf{p}}(\tau) = \int d^3x e^{-i\mathbf{p}\cdot\mathbf{x}} u(\tau, \mathbf{x}). \quad (7)$$

From the Lagrangian (3), we obtain a Bogoliubov–de Gennes (BdG) system in the momentum

space

$$u''_{\mathbf{p}} + \Omega_p^2(\tau)u_{\mathbf{p}} + R(\tau)u_{-\mathbf{p}}^* = 0 \quad (8)$$

$$u''^*_{\mathbf{p}} + \Omega_p^2(\tau)u_{\mathbf{p}}^* + R^*(\tau)u_{-\mathbf{p}} = 0 \quad (9)$$

with

$$\Omega_p^2(\tau) = p^2 + a^2(m^2 + \mu^2) - \frac{a''}{a}, \quad R(\tau) \equiv \frac{A^2}{H^2\tau^2}(-H\tau)^{-2i\mu/H} \quad (10)$$

Here  $R$  contains both the amplitude  $A^2a^2$  and the time-dependent phase inherited from the chemical potential. For exact de Sitter,  $a(\tau) = -1/(H\tau)$  and  $e^{\pm 2i\mu t} = (-H\tau)^{\mp 2i\mu/H}$ , so  $\arg[R(\tau)] = -(2\mu/H)\ln(-H\tau)$ .

It is instructive to decompose the  $\chi$  field into its real and imaginary part. Writing  $u = (u_+ + u_-)/\sqrt{2}$ , one finds

$$u''_+ + \left[ k^2 + \frac{m^2 + \mu^2}{H^2\tau^2} - \frac{2}{\tau^2} + \frac{A^2}{H^2\tau^2} \cos \theta(\tau) \right] u_+ - \frac{A^2}{H^2\tau^2} \sin \theta(\tau) u_- = 0, \quad (11)$$

$$u''_- + \left[ k^2 + \frac{m^2 + \mu^2}{H^2\tau^2} - \frac{2}{\tau^2} - \frac{A^2}{H^2\tau^2} \cos \theta(\tau) \right] u_- - \frac{A^2}{H^2\tau^2} \sin \theta(\tau) u_+ = 0. \quad (12)$$

where  $\theta(\tau) = (2\mu/H)\ln(-H\tau)$ . There are two limits that clarify the dynamics:

- $\mu \rightarrow 0$  (*no chemical potential*): the off-diagonal terms that proportion to  $\sin \theta$  vanish and  $u_{\pm}$  decouple. For sufficiently large  $A/H$ , the  $u_-$  sector can develop a tachyonic window, which is the familiar instability of complex-scalar models with strong  $U(1)$  breaking.
- $\mu \neq 0$  (*our case*) the diagonal frequencies are raised by  $\mu^2$ , shrinking or eliminating broad tachyonic bands, while the  $u_+$ - $u_-$  mixing oscillates in time. Production is then dominated by phase-matched resonances rather than by a sustained tachyonic roll.

**Instantaneous super-adiabatic basis** To compute particle production cleanly we expand in an instantaneous super-adiabatic basis [48, 49] with a positive frequency  $W_p(\tau)$ :

$$f_p^{\pm}(\tau) = \frac{1}{\sqrt{2W_p(\tau)}} e^{\mp i\theta_p(\tau)}, \quad \theta_p(\tau) \equiv \int^{\tau} W_p(\tilde{\tau}) d\tilde{\tau} \quad (13)$$

and decompose

$$u_{\mathbf{p}}(\tau) = \alpha_{\mathbf{p}}(\tau) f_p^+(\tau) + \beta_{\mathbf{p}}(\tau) f_p^-(\tau), \quad (14)$$

$$u_{-\mathbf{p}}^*(\tau) = \alpha_{-\mathbf{p}}^*(\tau) f_p^-(\tau) + \beta_{-\mathbf{p}}^*(\tau) f_p^+(\tau), \quad (15)$$

which enforce  $|\alpha_{\mathbf{p}}|^2 - |\beta_{\mathbf{p}}|^2 = 1$  at all times. The frequency  $W_p(\tau)$  satisfy the differential equation,

$$W_p^2 = \Omega_p^2 - \frac{1}{2} \frac{W_p''}{W_p} + \frac{3}{4} \left( \frac{W_p'}{W_p} \right)^2 \quad (16)$$

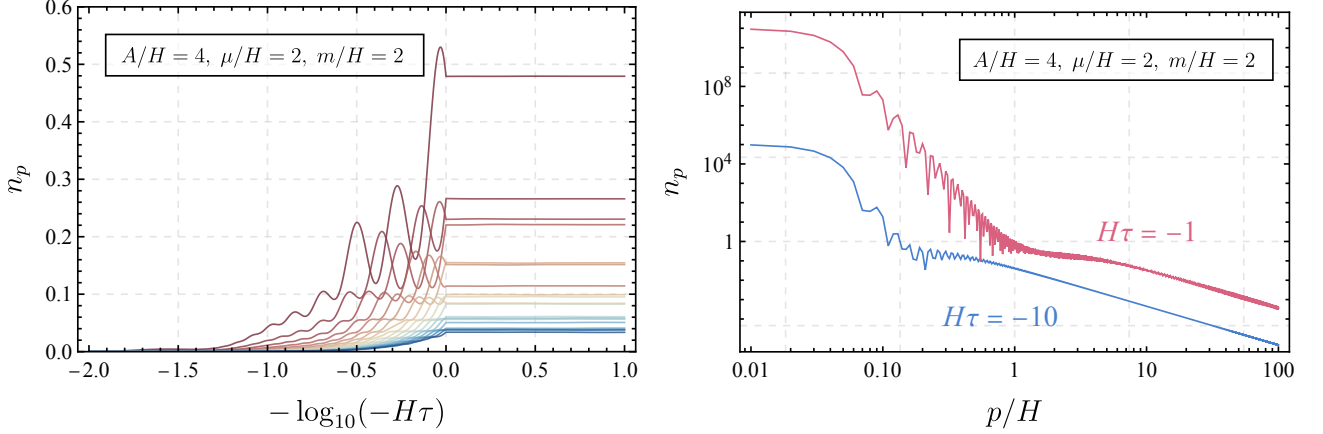


Figure 2: *Left panel*: The evolution of the comoving phase space number density of various mode with momentum range from  $p/H \in (1, 7)$ , where blue/red denote mode with large/small momentum. *Right panel*: The comoving phase space distribution at given comoving time  $H\tau = -1$  and  $H\tau = -0.5$ . The rapid oscillation of  $n_p$  is evident in this plot.

Based on the convergence of the fixed-point iteration,  $W_p$  can be determined using the following iterative scheme:

$$(W_p^{(j+1)})^2 = \Omega_p^2 - \frac{1}{2} \frac{(W_p^{(j)})''}{W_p^{(j)}} + \frac{3}{4} \left( \frac{(W_p^{(j)})'}{W_p^{(j)}} \right)^2 \quad (17)$$

In this section, we adopt the super-adiabatic basis defined by the frequency  $W_p = W_p^{(1)}$  to accurately describe the evolution of the number density and to delineate the boundaries of the viable parameter space. For the gravitational wave computation detailed in the subsequent section, we utilize the leading-order adiabatic approximation,  $(W_p^{(0)})^2 = \Omega_p^2$ . This simplification is implemented to ensure numerical stability, given that the impact of higher-order adiabatic corrections on the final tensor power spectrum to be negligible. The occupation number per-mode of the  $\chi$  quanta is determined by the Bogoliubov coefficient  $\beta_{\mathbf{p}}$  through  $n_{\mathbf{p}}(\tau) = |\beta_{\mathbf{p}}(\tau)|^2$ . Collecting  $\Psi_{\mathbf{p}} \equiv (\alpha_{\mathbf{p}}, \beta_{\mathbf{p}}, \alpha_{-\mathbf{p}}^*, \beta_{-\mathbf{p}}^*)^T$ , one obtains the compact first-order system

$$\Psi'_{\mathbf{p}} = \begin{pmatrix} \delta & (\Delta + \delta)e^{2i\theta} & \gamma e^{2i\theta} & \gamma \\ (\Delta - \delta)e^{-2i\theta} & -\delta & -\gamma & -\gamma e^{-2i\theta} \\ \gamma^* e^{-2i\theta} & \gamma^* & \delta^* & (\Delta + \delta^*)e^{-2i\theta} \\ -\gamma^* & -\gamma^* e^{2i\theta} & (\Delta - \delta^*)e^{2i\theta} & -\delta^* \end{pmatrix} \Psi_{\mathbf{p}}. \quad (18)$$

with  $\Delta$ ,  $\delta$  and  $\gamma$  defined in appendix A. The Bunch–Davies initial condition  $\alpha_p(-\infty) = 1$ ,  $\beta_p(-\infty) = 0$  selects the adiabatic vacuum in the asymptotic past. Numerically (see Figure 2) one observes that  $n_{\mathbf{p}}(\tau)$  exhibits oscillatory feature with frequency proportion to the effective chemical  $\mu$  in physical time, precisely what one expects from a controlled, pump-driven production mechanism.

### 3.1 Constraints on the parameters

The resonant production of  $\chi$  generically injects a substantial amount of energy into the  $\chi$  sector. If too large, this backreaction can modify the inflationary background and invalidate the spectator approximation. Independently of these concerns, particle production must cease before the end of inflation. Therefore, as argued in Section 2, we assume the  $U(1)$ -breaking channel exists during the finite interval  $(\tau_i, \tau_*)$ . For a quadratic system, the produced energy density at  $\tau_*$  is, to leading adiabatic order,

$$\rho_\chi(\tau_*) = \frac{g_\chi}{2\pi^2 a^4(\tau_*)} \int_0^{a(\tau_*)\Lambda} dp \, p^2 W_p(\tau_*) n_p(\tau_*), \quad (19)$$

where  $n_p = |\beta_p|^2$  is the occupation number in the same (first-order) adiabatic basis used to define the instantaneous frequency  $W_p \equiv W_p^{(1)}$ , and  $\Lambda$  is the EFT's physical cutoff. Here, we take  $g_\chi = 1$  since  $n_p$  in the solution already combines both charges. As argued, We quantify backreaction by

$$f_\chi(\tau_*) \equiv \frac{\rho_\chi(\tau_*)}{\rho_{\text{inf}}} , \quad \rho_{\text{inf}} = 3M_{\text{Pl}}^2 H^2, \quad (20)$$

and require  $f_\chi(\tau_*) \ll 1$  throughout the parameter scans (Figure 3). This condition defines the region where the spectator treatment and the GW calculation are self-consistent. Figure 3 shows that a nonzero chemical potential markedly enlarges the viable region with  $A > m$ , permitting large resonant contributions while preserving slow-roll inflation. In Figure 3, the upper-left region corresponds to  $f_\chi > 1$ , indicating that the inflationary condition is violated prior to  $\tau_*$ . By contrast, the lower-right region yields  $f_\chi \ll 1$  consistent with maintaining inflation up to (and at)  $\tau_*$ . An interesting feature illustrated in Fig. (3) is that even in the region  $A^2 < m^2 + \mu^2 \equiv M_{\text{eff}}^2$ , particles are still efficiently produced via parametric resonance induced by the oscillating  $U(1)$ -breaking term.

## 4 The gravitational wave from the particle production

We work in the weak-gravity regime  $H/M_{\text{Pl}} \ll 1$ , treating the FRW background classically and quantizing only the linear tensor perturbation. In a spatially flat FRW spacetime with line element  $ds^2 = a^2(\tau) [-d\tau^2 + (\delta_{ij} + h_{ij})dx^i dx^j]$ , decompose the transverse-traceless(TT) metric perturbation into circular helicities,

$$h_{ij}(\mathbf{k}, \tau) = \sum_{\lambda=\pm} e_{ij}^\lambda(\hat{\mathbf{k}}) h_\lambda(\mathbf{k}, \tau), \quad (21)$$

where  $k^i e_{ij}^\lambda = 0$ ,  $e_{ii}^\lambda = 0$ , and  $e_{ij}^\lambda(\hat{\mathbf{k}}) e_{ij}^{\lambda'}(\hat{\mathbf{k}}) = 2\delta_{\lambda\lambda'}$ . Spatial indices are raised/lowered with  $\delta_{ij}$ , and a prime denotes  $\partial/\partial\tau$ . We denote the conformal Hubble rate by  $\mathcal{H} \equiv a'/a$ ; during exact de Sitter  $a(\tau) = -1/(H\tau)$  (with  $H$  constant) and hence  $\mathcal{H} = -1/\tau$ . The helicity modes obey the sourced tensor equation

$$h_\lambda'' + 2\mathcal{H}h_\lambda' + k^2 h_\lambda = \frac{2}{M_{\text{Pl}}^2} a^2(\tau) S_\lambda(\mathbf{k}, \tau) \quad (22)$$

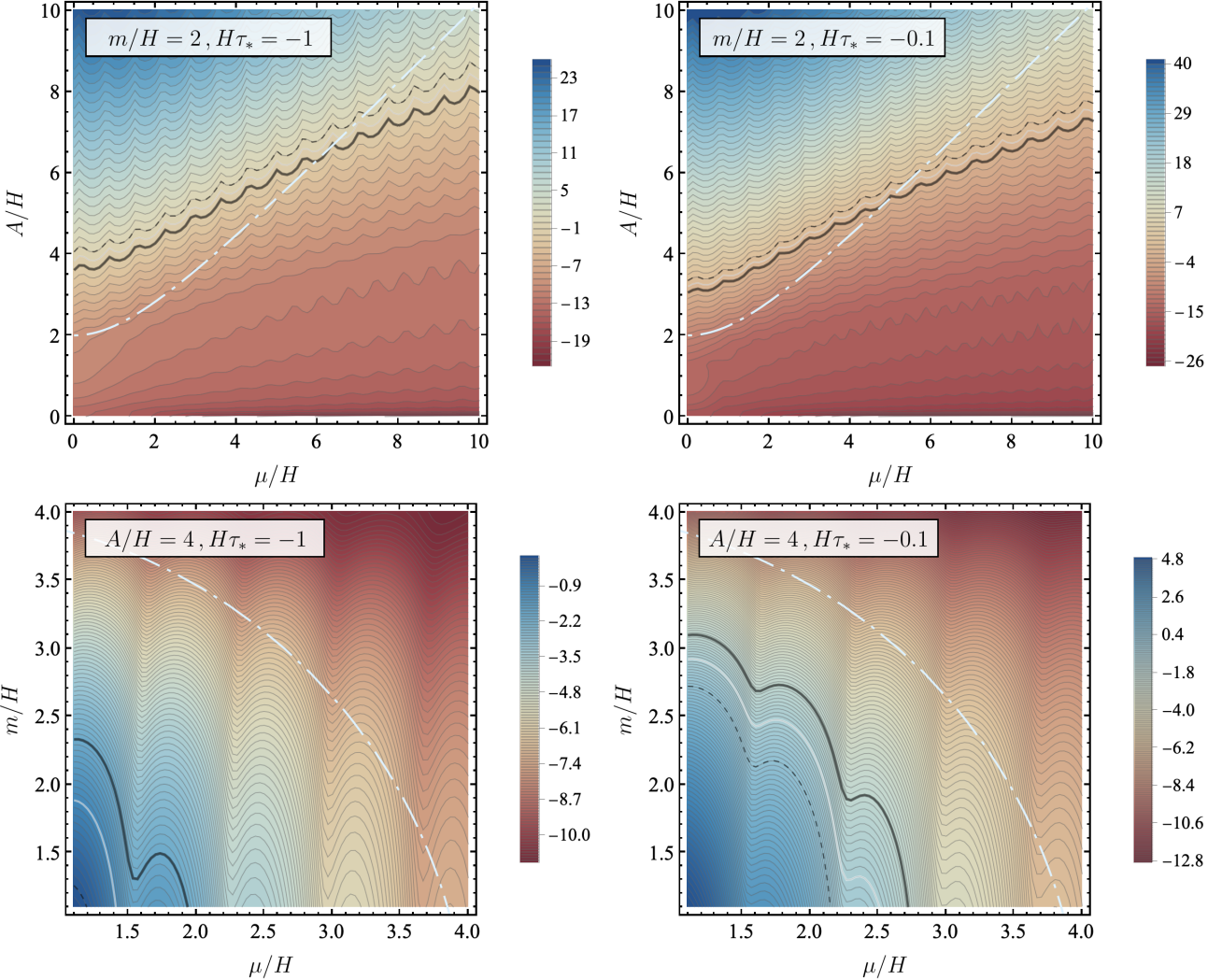


Figure 3: Constraints on the  $(\mu/H, A/H)$  and  $(\mu/H, m/H)$  planes with  $H\tau_i = -100$ , where color indicates  $\log_{10} f_\chi$ . The solid black, solid white, and dashed curves mark the contours  $f_\chi = 0.01, 0.1, 1$  respectively. The dot-dashed curve denote the contour where  $A^2 = m^2 + \mu^2$ .

with source

$$S_\lambda(\mathbf{k}, \tau) \equiv e_{ij}^\lambda(\hat{\mathbf{k}}) \Pi_{ij}(\mathbf{k}, \tau), \quad \Pi_{ij} \equiv T_{ij}^{(\chi)} - \frac{1}{3} \delta_{ij} T_{\ell\ell}^{(\chi)}, \quad (23)$$

the TT anisotropic stress of the spectator field. In the Fourier convention used above, the (spatial) stress tensor of a scalar gives

$$T_{ij}^{(\chi)}(\mathbf{k}) = \int \frac{d^3 p}{(2\pi)^3} [p_i(p-k)_j + p_j(p-k)_i] \chi_{\mathbf{p}} \chi_{\mathbf{p}-\mathbf{k}}^* - \delta_{ij}(\text{trace}), \quad (24)$$

and the helicity-projected source can be written as

$$S_\lambda(\mathbf{k}, \tau) = 2 \int \frac{d^3 p}{(2\pi)^3} E_\lambda(\mathbf{p}, \mathbf{k}) \chi_{\mathbf{p}} \chi_{\mathbf{k}-\mathbf{p}}^*, \quad (25)$$

with TT kernel

$$E_\lambda(\mathbf{p}, \mathbf{k}) \equiv e_{ij}^\lambda(\hat{\mathbf{k}}) p_i (k_j - p_j) = -e_{ij}^\lambda(\hat{\mathbf{k}}) p_i p_j. \quad (26)$$

The second equality follows from transversality  $k^i e_{ij}^\lambda = 0$ . Throughout this section and the following sections,  $\chi$  denotes the spectator field after the time-dependent phase rotation used in Sec 2 to remove the chemical potential; the TT projection of  $T_{ij}^{(\chi)}$  is unchanged by this field redefinition.

To solve (22) we introduce the retarded Green's function  $G_k(\tau, \tau')$  defined by

$$(\partial_\tau^2 + 2\mathcal{H}(\tau)\partial_\tau + k^2) G_k(\tau, \tau') = \delta(\tau - \tau'), \quad G_k(\tau < \tau', \tau') = 0. \quad (27)$$

In exact de Sitter one finds the closed form

$$G_k(\tau, \tau') = -\Theta(\tau - \tau') \frac{(k\tau - k\tau') \cos[k(\tau - \tau')] - (1 + k^2\tau\tau') \sin[k(\tau - \tau')]}{k^3\tau'^2}, \quad (28)$$

which satisfies the jump condition  $G'_k(\tau' + 0, \tau') = 1$  implied by (27). For quasi-de Sitter, slow-roll corrections to (28) are subleading for our purposes.

The solution to (22) is then

$$h_\lambda(\mathbf{k}, \tau) = \frac{2}{M_{\text{Pl}}^2} \int_{-\infty}^{\tau} d\tau' G_k(\tau, \tau') a^2(\tau') S_\lambda(\mathbf{k}, \tau') \quad (29)$$

which will be the starting point for the renormalized two-point function and the tensor power spectrum in the next section.

## 4.1 The gravitational wave power spectrum

As previously discussed, the helicity source entering the tensor equation is the TT projection of the spectator stress given in (25). We will use this to determine the time ordering in the two-point kernels below. The source  $S_\lambda$  is quadratic in the quantum field  $\chi$  and requires renormalization [50–53]. We adopt covariant point-splitting with adiabatic subtraction and define the renormalized quadratic composite by

$$(\partial_i \chi \partial_j \chi^*)_{\text{ren}}(x) = \lim_{y \rightarrow x} \left[ \partial_i \chi(x) \partial_j \chi^*(y) - \partial_i \partial_j F_{\text{ad}}^{(\chi)}(x, y) \right]. \quad (30)$$

with  $F_{\text{ad}}^{(\chi)}(x, y) \equiv \langle 0_{\text{ad}} | \chi(x) \chi^*(y) | 0_{\text{ad}} \rangle$ . In momentum space this becomes  $\partial_i \partial_j F_{\text{ad}}^{(\chi)} \rightarrow p_i(k_j - p_j) F_{\text{ad}}^{(\chi)}(p; \tau, \tau')$ . Using  $u = a\chi$ , the adiabatic subtractor is

$$F_{\text{ad}}^{(\chi)}(p; \tau, \tau') = \frac{f_+^u(p, \tau) f_+^{u*}(p, \tau')}{a(\tau) a(\tau')}, \quad (31)$$

with  $f_\pm^u = e^{-\mp \int^\tau W_p} / \sqrt{2W_p(\tau)}$  as defined in Sec 3. With this prescription, the renormalized helicity source in momentum space is

$$S_\lambda^{\text{ren}}(\mathbf{k}, \tau) = 2 \int \frac{d^3 \mathbf{p}}{(2\pi)^3} E_\lambda(\mathbf{p}, \mathbf{k}) \left[ \chi_{\mathbf{p}}(\tau) \chi_{\mathbf{k}-\mathbf{p}}^*(\tau) - (2\pi)^3 \delta^{(3)}(\mathbf{k}) F_{\text{ad}}^{(\chi)}(p; \tau, \tau) \right], \quad (32)$$

so that  $\langle S_\lambda^{\text{ren}} \rangle = 0$  and UV divergences in the two-point function are subtracted by  $F_{\text{ad}}^{(\chi)}$ . The observable tensor power spectrum is defined by the variance of  $h_\lambda$ ,

$$P_h(k, \tau) = \frac{k^3}{\pi^2} \sum_{\lambda=\pm} \langle |h_\lambda(\mathbf{k}, \tau)|^2 \rangle, \quad (33)$$

which requires the connected two-point function of  $S_\lambda^{\text{ren}}$ . Using Wick's theorem and (31), (32) the connected correlator (up to local contact terms that only renormalize geometric coupling) is,

$$\begin{aligned} \langle S_\lambda^{\text{ren}}(\mathbf{k}, \tau') S_{\lambda'}^{\text{ren}}(\mathbf{k}', \tau'') \rangle &= (2\pi)^3 \delta^{(3)}(\mathbf{k} + \mathbf{k}') \delta_{\lambda\lambda'} \\ &\times 4 \int \frac{d^3 \mathbf{p}}{(2\pi)^3} |E_\lambda(\mathbf{p}, \mathbf{k})|^2 F_{\text{ren}}^{(\chi)}(p; \tau', \tau'') F_{\text{ren}}^{(\chi)}(|\mathbf{k} - \mathbf{p}|; \tau', \tau''). \end{aligned} \quad (34)$$

Here,

$$F_{\text{ren}}^{(\chi)}(p; \tau, \tau') \equiv \langle \text{BD} | \chi_p(\tau) \chi_p^*(\tau') | \text{BD} \rangle - F_{\text{ad}}^{(\chi)}(p; \tau, \tau') \quad (35)$$

is the renormalized two-point kernel built from the BD state specified in the asymptotic past. The tensor solution from

$$h_\lambda(\mathbf{k}, \tau) = \frac{2}{M_{\text{Pl}}^2} \int_{-\infty}^{\tau} d\tau' G_k(\tau, \tau') a^2(\tau') S_\lambda(\mathbf{k}, \tau') \quad (36)$$

together with the expression for the source correlator (34), gives

$$\begin{aligned} P_h(k, \tau) &= \frac{16k^3}{\pi^2 M_{\text{Pl}}^4} \int_{-\infty}^{\tau} d\tau' \int_{-\infty}^{\tau} d\tau'' a^2(\tau') a^2(\tau'') G_k(\tau, \tau') G_k(\tau, \tau'') \\ &\times \int \frac{d^3 \mathbf{p}}{(2\pi)^3} \sum_{\lambda=\pm} |E_\lambda(\mathbf{p}, \mathbf{k})|^2 F_{\text{ren}}^{(\chi)}(p; \tau', \tau'') F_{\text{ren}}^{(\chi)}(|\mathbf{k} - \mathbf{p}|; \tau'', \tau'). \end{aligned} \quad (37)$$

Using the canonical basis of Sec 3 and  $u = a\chi$ , the field expansion reads

$$\chi_p(\tau) = \frac{1}{a(\tau)} \left[ f_+^u(p, \tau) b_p(\tau) + f_-^u(p, \tau) b_{-p}^\dagger(\tau) \right], \quad b_p = \alpha_p a_p + \beta_p a_{-p}^\dagger, \quad (38)$$

with  $|\alpha_p|^2 - |\beta_p|^2 = 1$  and  $n_p = |\beta_p|^2$ . A short computation gives the BD two-point function

$$\begin{aligned} \langle \chi_p(\tau') \chi_p^*(\tau'') \rangle &= \frac{1}{a(\tau') a(\tau'')} \left[ f_+^u(\tau') f_+^{u*}(\tau'') \alpha_p(\tau') \alpha_p^*(\tau'') + f_-^u(\tau') f_-^{u*}(\tau'') \beta_p(\tau') \beta_p^*(\tau'') \right. \\ &\quad \left. + f_+^u(\tau') f_-^{u*}(\tau'') \alpha_p(\tau') \beta_p^*(\tau'') + f_-^u(\tau') f_+^{u*}(\tau'') \beta_p(\tau') \alpha_p^*(\tau'') \right], \end{aligned} \quad (39)$$

and, subtracting the adiabatic vacuum,

$$\begin{aligned} F_{\text{ren}}^{(\chi)}(p; \tau', \tau'') &= \frac{1}{a(\tau') a(\tau'')} \left[ f_+^u(\tau') f_+^{u*}(\tau'') (\alpha_p(\tau') \alpha_p^*(\tau'') - 1) + f_-^u(\tau') f_-^{u*}(\tau'') \beta_p(\tau') \beta_p^*(\tau'') \right. \\ &\quad \left. + f_+^u(\tau') f_-^{u*}(\tau'') \alpha_p(\tau') \beta_p^*(\tau'') + f_-^u(\tau') f_+^{u*}(\tau'') \beta_p(\tau') \alpha_p^*(\tau'') \right]. \end{aligned} \quad (40)$$

Throughout the calculation of  $P_h$  we approximate the renormalized two-point function of the source field by neglecting the contribution from the second line of (40). This form follows

from the exact decomposition after adiabatic subtraction by retaining the pieces with phases  $e^{\pm i[\theta(\tau') - \theta(\tau'')]}$  and (ii) dropping the “sum-phase” coherence terms  $e^{\pm i[\theta(\tau') + \theta(\tau'')]}$  which are suppressed by non-stationary phase in the  $\tau'$ ,  $\tau''$  integrals. Therefore the two-point function in our calculation of the spectrum in the following is,

$$F_{\text{ren}}^{(X)}(p; \tau', \tau'') \simeq \frac{(\alpha_p(\tau')\alpha_p^*(\tau'') - 1)e^{-i\int_{\tau''}^{\tau'} W_p} + \beta_p(\tau')\beta_p^*(\tau'')e^{+i\int_{\tau''}^{\tau'} W_p}}{2a(\tau')a(\tau'')\sqrt{W_p(\tau')W_p(\tau'')}}. \quad (41)$$

With (41), the final expression for the power spectrum becomes,

$$\begin{aligned} P_h^{\text{prim}}(k) &= \frac{16k}{\pi^2 M_{\text{Pl}}^4} \int_{-\infty}^0 d\tau' \int_{-\infty}^0 d\tau'' j_1(k\tau') j_1(k\tau'') \\ &\times \frac{1}{2\pi^2} \int_0^\infty dp p^6 \int_{-1}^1 ds (1-s^2)^2 \frac{1}{4\sqrt{W_p(\tau')W_p(\tau'')W_q(\tau')W_q(\tau'')}} \\ &\times \left[ [\alpha_p(\tau')\alpha_p^*(\tau'') - 1]e^{-i\Delta\theta_p} + \beta_p(\tau')\beta_p^*(\tau'')e^{+i\Delta\theta_p} \right] \\ &\times \left[ [\alpha_q(\tau')\alpha_q^*(\tau'') - 1]e^{+i\Delta\theta_q} + \beta_q(\tau')\beta_q^*(\tau'')e^{-i\Delta\theta_q} \right]. \end{aligned} \quad (42)$$

with  $q = \sqrt{k^2 + p^2 - 2kps}$  and  $\Delta\theta_{p,q}(\tau', \tau'') = \int_{\tau''}^{\tau'} W_{p,q}(\tilde{\tau}) d\tilde{\tau}$ , with  $s \equiv \cos\theta$  comes from the three dimensional momentum integral. In appendix B, we argue that the rapidly oscillating phase in (42) enable us to employ the stationary phase approximation, under which the power spectrum takes the form of

$$P_h^{\text{prim}}(k) \simeq \frac{8}{\pi^3 M_{\text{Pl}}^4} \int_{-\infty}^0 d\tau j_1^2(k\tau) \int_{k/2}^\infty dp p^6 \frac{1}{|W'(p; \tau)|} \left(1 - \frac{k^2}{4p^2}\right)^2 \frac{n_p^2(\tau)}{W_p^2(\tau)}. \quad (43)$$

Note that the lower bound of the  $\tau$  integral is extended to  $-\infty$ , which is reasonable since before  $\tau_i$  when the  $U(1)$ -breaking term is present, the produced particle number is exponentially suppressed in that regime.

## 4.2 From primordial power spectrum to the observable

In this section we translate the renormalized, time-dependent tensor power spectrum  $P_h(k, \tau)$  obtained in the previous sections into the present-day fractional energy density in gravitational waves,  $\Omega_{\text{GW},0}(f)$ , which is the target of PTA, LISA and ground-based interferometers [54–57]. To avoid any notational ambiguities, we now distinguish clearly between  $H(t) \equiv \dot{a}/a$  for the *physical* Hubble rate (entering  $\rho_c = 3M_{\text{Pl}}^2 H^2$ ), and  $\mathcal{H}(\tau) \equiv a'/a$  for the *conformal* Hubble rate; a dot (prime) denotes a derivative with respect to cosmic (conformal) time. We set today’s scale factor to unity,  $a_0 \equiv a(\tau_0) = 1$ , so that the present day physical frequency is  $f = k/(2\pi)$ .

Deep inside the horizon the effective stress-energy carried by the TT metric perturbation  $h_{ij}$  yields (in conformal time)

$$\rho_{\text{GW}}(\tau) = \frac{M_{\text{Pl}}^2}{4a^2} \left\langle h'_{ij} h'_{ij} + (\partial_\ell h_{ij})(\partial_\ell h_{ij}) \right\rangle. \quad (44)$$

Consequently, the spectral energy density per logarithmic wavenumber is

$$\frac{d\rho_{\text{GW}}}{d\ln k} = \frac{M_{\text{Pl}}^2}{4a^2} \frac{k^3}{2\pi^2} \sum_{\lambda=\pm} \left( |h'_\lambda|^2 + k^2 |h_\lambda|^2 \right), \quad (45)$$

and the (instantaneous) energy fraction in GWs becomes

$$\Omega_{\text{GW}}(k, \tau) \equiv \frac{1}{\rho_c} \frac{d\rho_{\text{GW}}}{d\ln k} = \frac{1}{12} \left( \frac{k}{aH} \right)^2 \overline{P_h(k, \tau)} \quad (46)$$

where the overline denotes an average over many oscillations and  $P_h$  is the dimensionless tensor power spectrum defined earlier in (33). Its expression in terms of the renormalized anisotropic-stress kernel of the spectator field and Green's functions was obtained in (37).

Let  $\tau_*$  denote a time after the source has switched off while the mode is still superhorizon. We define the primordial (superhorizon) tensor spectrum

$$P_h^{\text{prim}}(k) \equiv \lim_{-k\tau \rightarrow 0^+} P_h(k, \tau) \Big|_{\tau \gtrsim \tau_*}. \quad (47)$$

Once a mode re-enters the Hubble radius,  $k = aH$ , it evolves freely and the solution for each helicity can be written as

$$h_\lambda(k, \tau) = h_\lambda^{\text{prim}}(k) \mathcal{T}_h(k, \tau), \quad P_h(k, \tau) = P_h^{\text{prim}}(k) |\mathcal{T}_h(k, \tau)|^2, \quad (48)$$

where  $\mathcal{T}_h$  is a tensor transfer function fixed by the background expansion (no additional sources are present after  $\tau_*$ ). For modes that re-enter during radiation domination (RD),  $a \propto \tau$  and  $\mathcal{H} = 1/\tau$ . The regular solution of the homogeneous tensor equation is

$$\mathcal{T}_h^{\text{(RD)}}(k, \tau) = j_0(k\tau) = \frac{\sin(k\tau)}{k\tau}. \quad (49)$$

Averaging over oscillations for  $k\tau \gg 1$ , one has  $\overline{j_0^2(k\tau)} \simeq [2(k\tau)^2]^{-1}$ . Substituting this and  $\mathcal{H} = 1/\tau$  into Eq. (46) yields the well-known RD plateau:

$$\Omega_{\text{GW}}(k, \tau) = \frac{1}{24} P_h^{\text{prim}}(k), \quad k\tau \gg 1 \text{ in RD} \quad (50)$$

i.e. once a mode has entered during RD,  $\Omega_{\text{GW}}(k, \tau)$  remains constant thereafter so long as the Universe stays RD. This applies to essentially all frequencies probed by PTAs ( $f \sim \text{nHz}$ ), LISA ( $f \sim \text{mHz}$ ), and LIGO/Virgo/KAGRA ( $f \sim 10^1 - 10^3 \text{Hz}$ ), which re-enter well before matter-radiation equality. For completeness, if a mode re-enters during matter domination (MD), the envelope of  $\Omega_{\text{GW}}$  decays  $\propto a^{-1}$  between horizon entry and equality, translating into a suppression  $\propto (k/k_{\text{eq}})^2$  relative to the RD plateau. This regime affects only extremely low frequencies  $f \lesssim f_{\text{eq}}$  and is irrelevant for the bands of interest here.

Gravitational waves redshift exactly as free radiation,  $\rho_{\text{GW}} \propto a^{-4}$ . The *total* radiation bath, however, changes due to Standard Model species becoming nonrelativistic. Entropy conservation implies  $aT g_{*s}^{1/3} = \text{const}$ , while  $\rho_r \propto g_* T^4 \propto g_* g_{*s}^{-4/3} a^{-4}$ . Between horizon entry (at temperature  $T_k$ ) and today one therefore finds

$$\frac{\rho_{\text{GW}}}{\rho_r} \Big|_{\tau_0} = \frac{\rho_{\text{GW}}}{\rho_r} \Big|_{T_k} \times \frac{g_*(T_k)}{g_*(T_0)} \left( \frac{g_{*s}(T_0)}{g_{*s}(T_k)} \right)^{4/3}. \quad (51)$$

Combining this with the RD plateau (50) and multiplying by today's radiation fraction  $\Omega_{r,0} \equiv \rho_{r,0}/\rho_{c,0}$  gives our master mapping:

$$\Omega_{\text{GW},0}(k) = \frac{\Omega_{r,0}}{24} P_h^{\text{prim}}(k) \underbrace{\frac{g_*(T_k)}{g_*(T_0)} \left( \frac{g_{*s}(T_0)}{g_{*s}(T_k)} \right)^{4/3}}_{\mathcal{A}_{g_*}(k)} \times \mathcal{T}_\nu^2(k) \times \mathcal{T}_{\text{eq}}^2(k) \quad (52)$$

where  $\mathcal{A}_{g_*}(k)$  encodes the Standard Model  $g_*$  and  $g_{*s}$  evolution between horizon entry and today;  $\mathcal{T}_\nu(k) \leq 1$  accounts for damping by free-streaming neutrinos (for modes that enter well before equality,  $\mathcal{T}_\nu$  approaches an  $\mathcal{O}(1)$  constant); and  $\mathcal{T}_{\text{eq}}(k)$  describes the additional suppression for modes that re-enter during MD (unity for  $k \gg k_{\text{eq}}$ ; approximately  $(k/k_{\text{eq}})$  in amplitude, hence  $(k/k_{\text{eq}})^2$  in power, for  $k \ll k_{\text{eq}}$ ).

### 4.3 Frequency mapping and the numerical results

To determine the physical frequency of a gravitational wave observed today, we use the CMB pivot mode as an observational anchor and then fix the relative redshift between the CMB mode and the GW mode of interest by exploiting the dark-matter relic abundance. Let  $N_*$  denote the number of e-folds of inflation that occur after the  $U(1)$ -breaking is switched off at time  $\tau_*$ . By definition (see (20)), the  $\chi$ -sector energy fraction at  $\tau_*$  is  $f_\chi^* \equiv \rho_\chi(\tau_*)/\rho_{\text{inf}}$ . Because non-relativistic  $\chi$  redshifts as  $a^{-3}$  while  $\rho_{\text{inf}}$  is approximately constant during slow roll, the energy fraction at the end of inflation is  $f_\chi^{(\text{end})} = f_\chi^* e^{-3N_*}$ . Assuming instantaneous reheating, the inflaton energy density is converted into radiation at temperature  $T_{\text{reh}}$ , and the comoving  $\chi$  yield at reheating is

$$Y_\chi \equiv \frac{n_\chi}{s} = \frac{\rho_\chi^{(\text{end})}/m_\chi}{s_{\text{reh}}} = \frac{3}{4} \left( \frac{g_*}{g_{*s}} \right) \frac{T_{\text{reh}}}{m_\chi} f_\chi^{(\text{end})} \quad (53)$$

The present  $\chi$  energy density is  $\rho_{\chi,0} = m_\chi s_0 Y_\chi$ . Using  $s_0 \simeq 2891.2 \text{ cm}^{-3}$  and  $\rho_{c,0}/h^2 \simeq 1.05 \times 10^{-5} \text{ GeV cm}^{-3}$ , the relic abundance becomes

$$\Omega_{\chi,0} h^2 = (2.06 \times 10^8 \text{ GeV}^{-1}) \left( \frac{g_*}{g_{*s}} \right)_{\text{reh}} \left( \frac{T_{\text{reh}}}{\text{GeV}} \right) f_\chi(\tau_*) e^{-3N_*} \quad (54)$$

which is independent of  $m_\chi$  because we have anchored the calculation to an energy fraction at production. Solving (54) for  $N_*$  with  $\Omega_{\chi,0} h^2 = 0.12$  yields

$$N_* \simeq 7.09 + \frac{1}{3} \ln \left( \frac{T_{\text{reh}}}{\text{GeV}} \right) + \frac{1}{3} \ln f_\chi^* \quad (55)$$

where we have used  $(g_*/g_{*s}) \simeq 1$  for high-temperature Standard-Model reheating. Next, we relate comoving scales to observed frequencies. Let  $N_{\text{CMB}}$  be the number of e-folds between horizon exit of the CMB pivot and the end of inflation ( $N_{\text{CMB}} \simeq 50 - 60$ ). The number of e-folds between the pivot's horizon exit and the switch-off time  $\tau_*$  is  $\Delta N \equiv N_{\text{CMB}} - N_*$ . Choose the  $k_*$  mode that exits the horizon at  $\tau_*$  as the reference mode, with approximately constant  $H$  during inflation, the horizon-exit condition  $k = aH$  implies  $k_*/k_{\text{CMB}} \simeq e^{\Delta N}$ . Since the present-day frequency scales as  $f \propto k$ , the physical frequency today of a mode with comoving momentum  $k$  is

$$f = f_{\text{CMB}} e^{\Delta N} \left( \frac{k}{k_*} \right) \quad (56)$$

where we take the Planck pivot  $k_{\text{CMB}} = 0.05 \text{ Mpc}^{-1}$ , corresponding to  $f_{\text{CMB}} \simeq 7.73 \times 10^{-17} \text{ Hz}$ . Therefore, the frequency of the reference mode  $k_*$  itself is  $f_* = f_{\text{CMB}} e^{\Delta N}$ . In the numerical illustrations below (Table 1), we present for several choices of the  $f_*$  for several choices of the  $U(1)$ -breaking amplitude  $A$ , fixing  $H = 10^{14} \text{ GeV}$ ,  $\mu/H = 2$ ,  $m/H = 2$  and  $H\tau_i = -100$ . These benchmarks are chosen to lie in the efficient yet small backreaction regime discussed earlier in the paper. In Figure 4 we show the characteristic shape of the numerically computed gravita-

$A/H$	$f_\chi^*$	$N_*$	$N_{\text{CMB}}$	$f_*$ (Hz)
4	$5.3 \times 10^{-4}$	16	55	6.0
4	$5.3 \times 10^{-4}$	16	60	900
4.5	0.135	18	50	$5.5 \times 10^{-3}$
4.5	0.135	18	60	122

Table 1: Benchmarks for the gravitational wave.

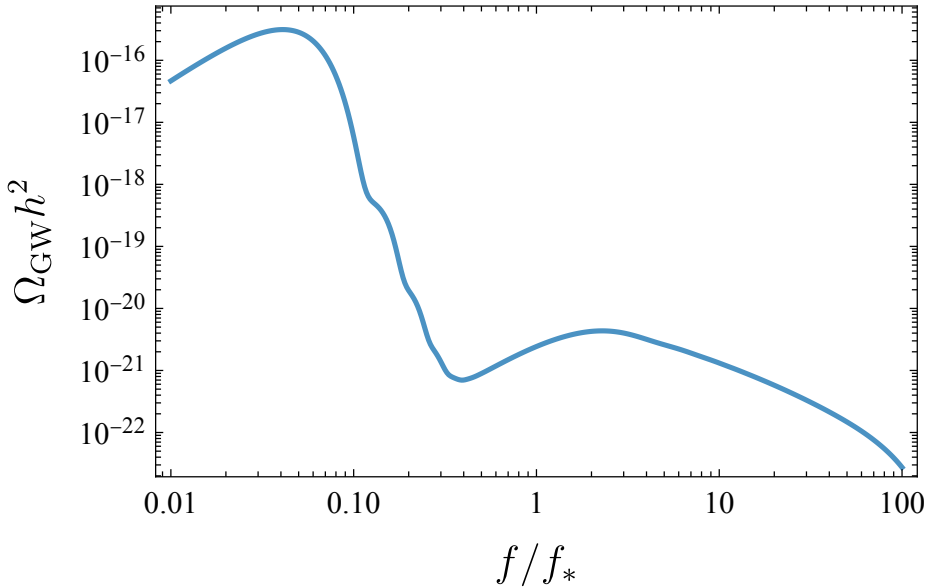


Figure 4: The shape of the gravitational wave energy density spectrum  $\Omega_{\text{GW}} h^2$  as a function of frequency  $f$  scaled by the frequency  $f_*$  of the reference mode.

tional wave energy density spectrum,  $\Omega_{\text{GW}}(f)$ . Figure 5 presents the spectrum obtained for the parameter choices listed in Table 1. Assuming that  $\chi$  constitutes the entire dark matter relic abundance and that reheating is instantaneous, these conditions fix the characteristic GW frequency. Under this benchmark, the predicted signal falls within the projected sensitivity curves of

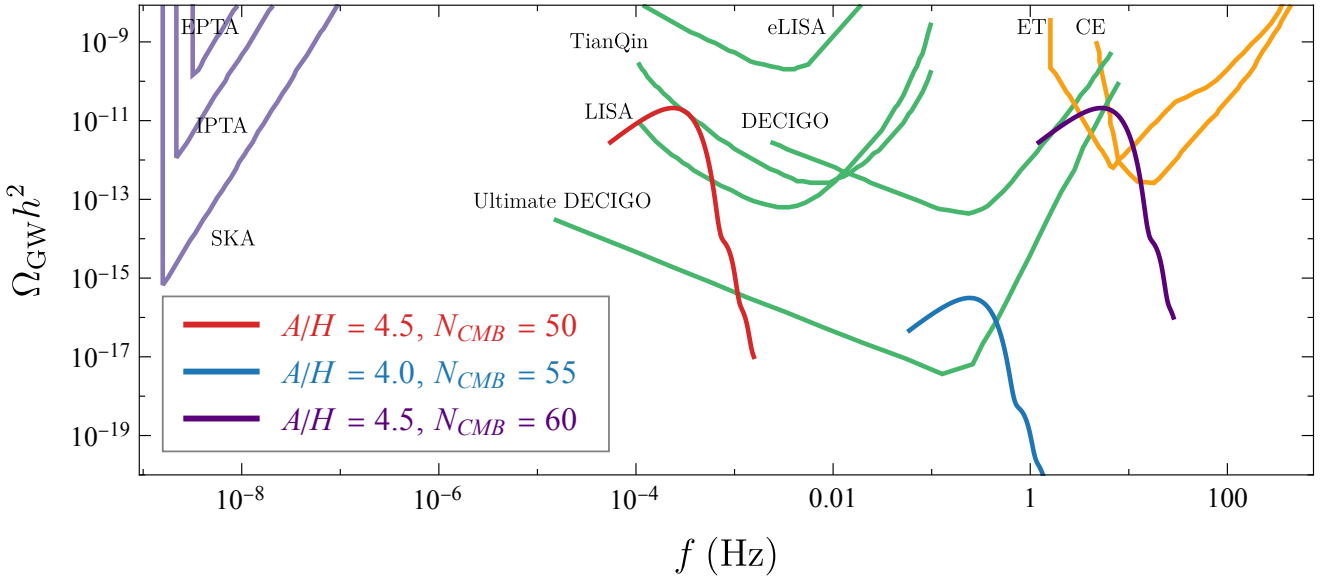


Figure 5: Gravitational wave energy density spectrum  $\Omega_{\text{GW}} h^2$  as a function of frequency  $f$  for the benchmark points listed in Table 1. For reference, we overlay representative projected sensitivity curves of selected ongoing and planned gravitational wave observatories.

space-based detectors (DECIGO [58], LISA [32], TianQin [33]) and next generation ground-based observatories (Einstein Telescope [59], Cosmic Explorer [60]).

## 5 The cosmological collider signal

In the previous sections we analyzed the stochastic gravitational-wave background sourced by resonant particle production, an intrinsically tensor observable. It has been shown [17] that the same dynamics imprints a scalar signature, an instance of cosmological-collider (CC) physics [46, 61–80], that is potentially observable in the CMB, large-scale structure (LSS), and forthcoming 21-cm surveys.

The CC perspective treats the inflationary Universe as a laboratory operating at a center-of-mass energy set by the Hubble scale  $H$ . Because the de Sitter horizon has an effective temperature  $T = H/(2\pi)$ , fields with masses  $m \lesssim \mathcal{O}(H)$  can be produced and subsequently interact with the inflaton perturbations. Their exchange leaves non-analytic features in inflationary correlators—most prominently in the bispectrum—whose oscillation frequency encodes particle masses while the angular dependence encodes spins. By analyzing these imprints we can infer the mass and spin of particles that were present during inflation, in close analogy with terrestrial colliders but at energies as high as  $H \sim 10^{14}$  GeV.

In our framework the complex scalar  $\chi$  experiences a derivative coupling  $\partial_\mu \phi J^\mu$  that induces an effective chemical potential  $\mu$ , together with a  $U(1)$ -breaking term  $A^2(\chi^2 + \chi^{*2})/2$ . After a time-dependent field rotation that removes the chemical term, the breaking operator acquires an oscillatory phase and acts as a coherent pump that mixes particle and antiparticle modes. This controlled non-adiabatic mixing both evades the usual Boltzmann suppression of heavy-field production and generates large occupation numbers, thereby sourcing the GW signal studied

earlier and, additionally, imprinting a distinctive, oscillatory non-Gaussianity in the curvature perturbation. The bispectrum is therefore an accessible CC probe in this model, with an amplitude governed by the same parameters  $(A, \mu, m)$  and backreaction fraction  $f_\chi$  that control the tensor signal. This CC signal is discussed extensively in [17]. The rest of this section review this CC prediction presented in [17].

Our model is endowed with a inflaton- $\chi$  coupling from the following expansion of the  $U(1)$ -breaking term, that is,

$$\chi^2 e^{-i\mu t - i\delta\phi/\Lambda} = (-\eta)^{i\mu/H} \left( 1 - i\frac{\delta\phi}{\Lambda} - \frac{\delta\phi^2}{2\Lambda^2} + \dots \right) \chi^2. \quad (57)$$

This give rise to the inflaton three point function corresponding to the processes depicted in the Feynman diagrams in Figure 6. The bispectrum is captured by a dimensionless quantity, which

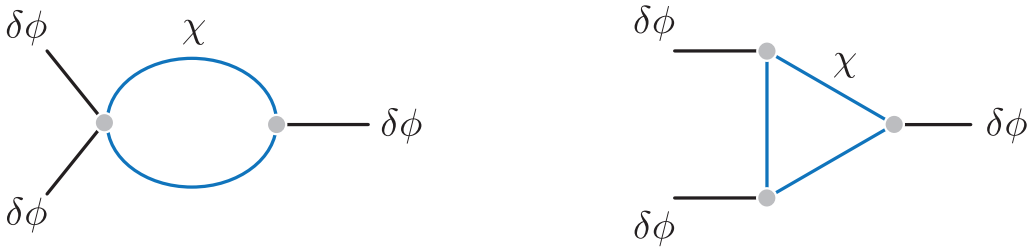


Figure 6: The Feynman diagrams that contributes to the bispectrum.

is conventionally defined as

$$S(k_1, k_2, k_3) = \frac{5}{6} \cdot \frac{\langle \zeta_{\mathbf{k}_1} \zeta_{\mathbf{k}_2} \zeta_{\mathbf{k}_3} \rangle'}{P_\zeta(k_1)P_\zeta(k_2) + P_\zeta(k_2)P_\zeta(k_3) + P_\zeta(k_3)P_\zeta(k_1)}, \quad (58)$$

where  $P_\zeta$  is the power spectrum and the prime on the correlator denotes the momentum conservation delta function is included implicitly. This quantity encodes the shape of the bispectrum and is thus called the shape function. Typically, the CC signal appears in the squeezed limit,  $k_3 \ll k_1 \sim k_2$ , in our case, it reads [17],

$$S_{\text{squeezed}}(k_1, k_2, k_3) \sim \frac{1}{16\pi^2} \left( \frac{\dot{\phi}_0}{H^2} \right) \left( \frac{A^2}{\Lambda H} \right)^2 \left( \frac{\mu/H}{\nu} \right) \left( \frac{k_1 + k_2}{2k_3} \right)^{-3+2i(\nu-\mu/H)} + \text{c.c.} \quad (59)$$

where  $M_{\text{eff}}^2 \equiv m^2 + \mu^2$  and  $\nu \equiv \sqrt{M_{\text{eff}}^2/H^2 - 9/4}$ . Note that this result is derived in the small  $A$  cases, where in a large  $A$  case, the occupation number may modify the expression in (59). The exact formula for the CC signal in the large  $U(1)$ -breaking case is beyond the scope of this work and we leave it for future studies. Nevertheless, it demonstrate that CC signal can serve as a cross validation for our model.

## 6 Conclusion and discussions

We have studied resonant production of a heavy  $U(1)$ -charged spectator during inflation, triggered by the interplay of a quadratic  $U(1)$ -breaking operator and an effective chemical potential  $\mu \equiv \dot{\phi}_0/\Lambda$  arising from a dimension-5 derivative coupling to the inflaton current. After

a time-dependent field rotation that removes the chemical term, the breaking operator acquires an oscillatory phase and acts as a coherent pump. This mechanism produces large occupation numbers of  $\chi$  particles without relying on broad tachyonic instabilities, and it remains efficient even in some regime where  $A < M_{\text{eff}}$ . We demonstrate the viable parameter space in Figure 3 that is consistent for the inflation.

A central phenomenological prediction is a sourced stochastic gravitational wave background generated by the anisotropic stress of the produced quanta. The resulting spectra, shown in Figure 5, can reside in the sensitivity bands of space-based detectors such as LISA/TianQin/DECIGO and next-generation ground-based observatories like ET/CE for realistic choices of the model parameters.

An appealing feature of the framework is its plausibility. Quadratic  $U(1)$ -breaking terms are ubiquitous, for example, SUSY  $b$ -terms [81], while the scalar chemical potential is the minimal EFT operator induced by a rolling inflaton. Within this setup the chemical potential lifts the diagonal mass, stabilizing against run-away tachyonic growth, while the time-dependent off-diagonal mixing supplies the required non-adiabaticity for resonant bursts. These properties make the mechanism predictive yet flexible.

The scenario also interfaces directly with two active lines of inquiry. First, there is strong, multi-band experimental interest in stochastic GW backgrounds—from pulsar-timing arrays in the nHz regime to planned space- and ground-based interferometers in the mHz–kHz range—precisely the window into which the produced particle of our model can account for the dominant constituent of the dark matter relic abundance. Second, the same couplings that drive production generically imprint a cosmological collider signal enabling a coherent multi-observable test that helps differentiate the mechanism from purely post-inflationary sources.

A natural next step is to test the mechanism in the fully nonlinear regime: lattice simulations [82] that include rescattering and backreaction can map when the spectator approximation breaks down, quantify departures from the  $n_{\chi}^2$  scaling implicit in the stationary-phase expression for the tensor power, and sharpen the boundary of the small-backreaction region highlighted in Figure (3), thereby validating the use of (43) for the subsequent mapping to  $\Omega_{\text{GW},0}(f)$  via (52). In parallel, the idealized sharp switch-on/off of the  $U(1)$ -breaking should be replaced by smooth, slow-roll-compatible triggers, e.g. a time-dependent  $\langle\sigma\rangle$  induced and later removed by a hybrid waterfall sector as in (6), and embedded in explicit UV completions such as SUSY  $b$ -terms or heavy-mediator EFTs generating  $\partial\phi J$ ; this would reveal how realistic profiles restructure the peak position, width, and normalization of the sourced spectrum while maintaining EFT control. A third avenue is to quantify a possible dissipative (warm-inflation-like) regime [83–87] when  $\chi$  self-interactions render scattering/thermalization rapid during production: computing dissipation coefficients (e.g. via Kubo relations), thermalization rates, and their feedback on slow roll will determine when additional friction is realized without spoiling the background and how it deforms both the primordial tensors and the frequency mapping tied to reheating. Finally, extending beyond a single complex scalar to fermions or gauge fields with analogous derivative couplings and explicit breaking, to multi-field flavor mixing, or to sectors with small sound speed—can uncover spin/statistics-dependent resonance patterns, altered polarization structure of the tensor source, and distinctive cosmological-collider imprints governed by the same microscopic parameters, offering orthogonal consistency checks of the framework within a common observational

pipeline.

## Acknowledgment

We thank Seung J. Lee and Chon Man Sou for useful discussions and for providing valuable comments on an earlier version of this manuscript. Research of Y.Y. is supported by the KIAS New Generation Research Program under Grant No. PG105801.

## A Evolution of the Bogoliubov coefficients

In this appendix we derive the time evolution of the Bogoliubov coefficients  $\alpha$  and  $\beta$  for the rescaled complex scalar field  $u$  obeying

$$u''_{\mathbf{p}} + \Omega_p^2(\tau) u_{\mathbf{p}} + R(\tau) u_{-\mathbf{p}}^* = 0, \quad (60)$$

$$u_{-\mathbf{p}}^{*''} + \Omega_p^2(\tau) u_{\mathbf{p}}^* + R^*(\tau) u_{-\mathbf{p}} = 0, \quad (61)$$

where  $' \equiv d/d\tau$  is the derivative with respect to conformal time. Following the main text, we decompose the modes in the adiabatic basis  $f^{\pm}$

$$u_{\mathbf{p}}(\tau) = \alpha_{\mathbf{p}}(\tau) f_p^+(\tau) + \beta_{\mathbf{p}}(\tau) f_p^-(\tau), \quad (62)$$

$$u_{-\mathbf{p}}^*(\tau) = \alpha_{-\mathbf{p}}^*(\tau) f_p^-(\tau) + \beta_{-\mathbf{p}}^*(\tau) f_p^+(\tau), \quad (63)$$

with

$$f_p^{\pm}(\tau) = \frac{1}{\sqrt{2W_p(\tau)}} e^{\mp i\theta_p(\tau)}, \quad \theta_p(\tau) \equiv \int^{\tau} W_p(\tilde{\tau}) d\tilde{\tau}, \quad (64)$$

and  $W_p(\tau)$  real. For readability we suppress the momentum label  $p$  of  $W$  and  $\Omega$  in below. We shall frequently use

$$f'_{\pm} = \left( -\frac{W'}{2W} \mp iW \right) f_{\pm}, \quad f''_{\pm} = \left[ -W^2 - \frac{W''}{2W} + \frac{3}{4} \left( \frac{W'}{W} \right)^2 \right] f_{\pm}, \quad (65)$$

$$f_- = e^{2i\theta} f_+, \quad f_+ = e^{-2i\theta} f_-. \quad (66)$$

**Gauge choice.** To fix the moving frame in the two-dimensional solution space, we impose the standard gauge condition

$$u'_{\mathbf{p}} = (-iW + V) \alpha_{\mathbf{p}} f^+ + (iW + V) \beta_{\mathbf{p}} f^-, \quad (67)$$

with a real function  $V(\tau)$ . Define

$$\Delta \equiv \frac{W'}{2W} + V, \quad Q_{\pm} \equiv \mp iW + V. \quad (68)$$

Then  $f'_{\pm} = (-\Delta + Q_{\pm}) f_{\pm}$  and the gauge condition becomes  $u'_{\mathbf{p}} = Q_+ \alpha_{\mathbf{p}} f_+ + Q_- \beta_{\mathbf{p}} f_-$ .

**First linear relation.** Differentiating (62) and matching to (67) gives the constraint

$$(\alpha'_{\mathbf{p}} - \Delta \alpha_{\mathbf{p}}) f_+ + (\beta'_{\mathbf{p}} - \Delta \beta_{\mathbf{p}}) f_- = 0. \quad (69)$$

**Second linear relation (using the EOM).** Differentiating (67), using  $f'_{\pm} = (-\Delta + Q_{\pm})f_{\pm}$ , and substituting  $u''_{\mathbf{p}}$  into (60), we obtain

$$-R(\alpha_{-\mathbf{p}}^* f_- + \beta_{-\mathbf{p}}^* f_+) = \left\{ Q_+(\alpha'_{\mathbf{p}} + \Delta \alpha_{\mathbf{p}}) + \mathcal{K} \alpha_{\mathbf{p}} \right\} f_+ + \left\{ Q_-(\beta'_{\mathbf{p}} + \Delta \beta_{\mathbf{p}}) + \mathcal{K} \beta_{\mathbf{p}} \right\} f_-, \quad (70)$$

where

$$\mathcal{K}_{\pm} \equiv Q'_{\pm} - 2Q_{\pm}\Delta + Q_{\pm}^2 + \Omega^2 \quad \Rightarrow \quad \mathcal{K}_+ = \mathcal{K}_- = \mathcal{K}, \quad (71)$$

and one checks explicitly that  $\mathcal{K}$  is real:

$$\mathcal{K} = \Omega^2 - W^2 + V' - \frac{W'}{W}V - V^2. \quad (72)$$

Taking the difference of the  $f_+$  and  $f_-$  pieces in (70) to eliminate the imaginary parts yields

$$iW \left[ (\alpha'_{\mathbf{p}} + \Delta \alpha_{\mathbf{p}}) f_+ - (\beta'_{\mathbf{p}} + \Delta \beta_{\mathbf{p}}) f_- \right] = (\mathcal{K} + 2V\Delta)(\alpha_{\mathbf{p}} f_+ + \beta_{\mathbf{p}} f_-) + R(\alpha_{-\mathbf{p}}^* f_- + \beta_{-\mathbf{p}}^* f_+). \quad (73)$$

Using  $\Delta = W'/(2W) + V$  one finds

$$\mathcal{K} + 2V\Delta = \Omega^2 - W^2 + V' + V^2. \quad (74)$$

Define

$$\delta \equiv \frac{\Omega^2 - W^2 + V' + V^2}{2iW}, \quad \gamma \equiv \frac{R}{2iW}. \quad (75)$$

Then we have the second relation

$$(\alpha'_{\mathbf{p}} + \Delta \alpha_{\mathbf{p}}) f_+ - (\beta'_{\mathbf{p}} + \Delta \beta_{\mathbf{p}}) f_- = 2\delta(\alpha_{\mathbf{p}} f_+ + \beta_{\mathbf{p}} f_-) - \frac{iR}{W}(\alpha_{-\mathbf{p}}^* f_- + \beta_{-\mathbf{p}}^* f_+). \quad (76)$$

**First-order system.** Adding and subtracting (69) and (76), and using  $f_{\mp} = e^{\pm 2i\theta} f_{\pm}$ , we obtain

$$\alpha'_{\mathbf{p}} = \delta \alpha_{\mathbf{p}} + (\Delta + \delta)e^{2i\theta} \beta_{\mathbf{p}} + \gamma \left( e^{2i\theta} \alpha_{-\mathbf{p}}^* + \beta_{-\mathbf{p}}^* \right), \quad (77)$$

$$\beta'_{\mathbf{p}} = (\Delta - \delta)e^{-2i\theta} \alpha_{\mathbf{p}} - \delta \beta_{\mathbf{p}} - \gamma \left( \alpha_{-\mathbf{p}}^* + e^{-2i\theta} \beta_{-\mathbf{p}}^* \right). \quad (78)$$

Collecting  $\Psi_{\mathbf{p}} \equiv (\alpha_{\mathbf{p}}, \beta_{\mathbf{p}}, \alpha_{-\mathbf{p}}^*, \beta_{-\mathbf{p}}^*)^T$ , the system can be written compactly as

$$\Psi'_{\mathbf{p}} = \begin{pmatrix} \delta & (\Delta + \delta)e^{2i\theta} & \gamma e^{2i\theta} & \gamma \\ (\Delta - \delta)e^{-2i\theta} & -\delta & -\gamma & -\gamma e^{-2i\theta} \\ \gamma^* e^{-2i\theta} & \gamma^* & \delta^* & (\Delta + \delta^*)e^{-2i\theta} \\ -\gamma^* & -\gamma^* e^{2i\theta} & (\Delta - \delta^*)e^{2i\theta} & -\delta^* \end{pmatrix} \Psi_{\mathbf{p}}. \quad (79)$$

When  $R \rightarrow 0$  (so  $\gamma \rightarrow 0$ ), the  $(\alpha_{\mathbf{p}}, \beta_{\mathbf{p}})$  sector reduces to the form of Eq. (2.17) in [49] (with  $\omega \rightarrow \Omega$ ) in the main text; choosing the “natural” gauge  $V = -W'/(2W)$  sets  $\Delta = 0$  and yields the anti-diagonal system analogous to Eq. (2.20) in [49]

## B The stationary phase approximation

In the main text, we have shown that the power spectrum of the primordial gravitational wave can be written as

$$\begin{aligned}
P_h^{\text{prim}}(k) &= \frac{16k}{\pi^2 M_{\text{Pl}}^4} \int_{-\infty}^0 d\tau' \int_{-\infty}^0 d\tau'' j_1(k\tau') j_1(k\tau'') \\
&\times \frac{1}{2\pi^2} \int_0^\infty dp p^6 \int_{-1}^1 ds (1-s^2)^2 \frac{1}{4\sqrt{W_p(\tau')W_p(\tau'')W_q(\tau')W_q(\tau'')}} \\
&\times \left[ [\alpha_p(\tau')\alpha_p^*(\tau'') - 1] e^{-i\Delta\theta_p} + \beta_p(\tau')\beta_p^*(\tau'') e^{+i\Delta\theta_p} \right] \\
&\times \left[ (\alpha_q(\tau')\alpha_q^*(\tau'') - 1) e^{+i\Delta\theta_q} + \beta_q(\tau')\beta_q^*(\tau'') e^{-i\Delta\theta_q} \right], \tag{80}
\end{aligned}$$

with  $q = \sqrt{k^2 + p^2 - 2kps}$  and  $\Delta\theta_{p,q}(\tau', \tau'') = \int_{\tau''}^{\tau'} W_{p,q}(\tilde{\tau}) d\tilde{\tau}$ , with  $s \equiv \cos\theta$  comes from the three dimensional momentum integral. In this appendix, we employ the stationary phase approximation to simplify (80). To proceed, we introduce the mean and difference of  $\tau'$  and  $\tau''$  as two new integration variables,  $\tau \equiv (\tau' + \tau'')/2$  and  $\Delta \equiv \tau' - \tau''$ . So, the measure remains unchanged, that is  $d\tau' d\tau'' = d\tau d\Delta$ . Over the short correlation time in  $\Delta$ , all slowly varying quantities may be evaluated at mean time  $\tau$ :

$$j_1(k\tau') j_1(k\tau'') \simeq j_1^2(k\tau) \tag{81}$$

$$W_{p,q}(\tau') \simeq W_{p,q}(\tau'') \simeq W_{p,q}(\tau) \tag{82}$$

$$\alpha_{p,q}(\tau')\alpha_{p,q}^*(\tau'') \simeq |\alpha_{p,q}(\tau)|^2 \tag{83}$$

$$\beta_{p,q}(\tau')\beta_{p,q}^*(\tau'') \simeq |\beta_{p,q}(\tau)|^2 \tag{84}$$

Moreover, to leading order in  $\Delta$ ,

$$\Delta\theta_{p,q} = \int_{\tau-\Delta/2}^{\tau+\Delta/2} W_{p,q}(\tilde{\tau}) d\tilde{\tau} \simeq W_{p,q}(\tau)\Delta \tag{85}$$

These are the standard stationary-phase approximation applied around  $\Delta = 0$ . Beyond which the integral is suppressed by the rapidly oscillating phase. Use the Bogoliubov identity  $|\alpha|^2 - |\beta|^2 = 1$ . At equal time,

$$|\alpha_{p,q}(\tau)|^2 - 1 = |\beta_{p,q}(\tau)|^2 = n_{p,q}(\tau) \tag{86}$$

and the phase factors become  $e^{\mp i\Delta\theta_{p,q}} \rightarrow e^{\mp iW_{p,q}(\tau)\Delta}$ . Thus each square bracket in the last two line of (80) simplifies to

$$\left[ \dots \right]_{p,q} \simeq n_{p,q}(\tau) (e^{-iW_{p,q}(\tau)\Delta} + e^{iW_{p,q}(\tau)\Delta}) = 2n_{p,q}(\tau) \cos(W_{p,q}(\tau)\Delta) \tag{87}$$

Meanwhile, the denominator of (80) can be written as

$$\frac{1}{4\sqrt{W_p(\tau')W_p(\tau'')W_q(\tau')W_q(\tau'')}} \simeq \frac{1}{4W_p(\tau)W_q(\tau)} \tag{88}$$

Hence the part of the integrand comes from the mode functions is simply

$$\frac{1}{4\sqrt{W_p(\tau')W_p(\tau'')W_q(\tau')W_q(\tau'')}} \left[ \dots \right]_p \left[ \dots \right]_q \simeq \frac{n_p(\tau)n_q(\tau)}{W_p(\tau)W_q(\tau)} \cos(W_p(\tau)\Delta) \cos(W_q(\tau)\Delta) \quad (89)$$

With the substitutions of (82) and (89) into (80), the  $(\tau', \tau'')$  integrals become

$$\int_{-\infty}^0 d\tau' \int_{-\infty}^0 d\tau'' \left( \dots \right) \simeq \int_{-\infty}^0 d\tau j_1^2(k\tau) \underbrace{\int_{-\infty}^{+\infty} d\Delta \cos(W_p(\tau)\Delta) \cos(W_q(\tau)\Delta)}_{\mathcal{T}_{pq}(\tau)} \quad (90)$$

Note that we have extend the  $\Delta$  integration to  $\mathbb{R}$ , which is harmless because the integral is sharply localized near  $\Delta = 0$ . The resulting  $\Delta$  integral defines a correlation time

$$\mathcal{T}_{pq}(\tau) \equiv \int_{-\infty}^{+\infty} d\Delta \cos(W_p(\tau)\Delta) \cos(W_q(\tau)\Delta) . \quad (91)$$

Under stationary phase approximation,

$$\int (\cos a\Delta) \cdot (\cos b\Delta) d\Delta = \frac{1}{2} \int [\cos((a-b)\Delta) + \cos((a+b)\Delta)] d\Delta \quad (92)$$

$$= \pi [\delta(a-b) + \delta(a+b)] \quad (93)$$

Because  $W_{pq} > 0$ , the  $\delta(a+b)$  term is ineffective, thus the correlation time can be approximated as,

$$\mathcal{T}_{pq}(\tau) \simeq \pi \delta(W_p(\tau) - W_q(\tau)) \quad (94)$$

which impose the diagonal condition  $p \simeq q$ . Now, the  $(p, s)$  integral in (80) becomes,

$$\int_0^\infty dp p^6 \int_{-1}^1 ds (1-s^2)^2 \frac{n_p(\tau)n_q(\tau)}{W_p(\tau)W_q(\tau)} \cdot \mathcal{T}_{pq}(\tau), \quad q = \sqrt{k^2 + p^2 - 2kps} \quad (95)$$

Note that at fixed  $k, p, \tau$ , the delta constraint  $\delta(W_p(\tau) - W_q(\tau))$  is an equation for  $s$  since the frequency  $W$  is strictly increasing with its momentum. So  $W_p = W_q$  implies  $p = q$ . This pins  $s$  to  $k^2 + p^2 - 2kps_* = k^2$ . Hence,

$$s_* = \frac{k}{2p}, \quad \text{with } p \geq k/2 \quad (96)$$

As the result, the  $s$  integral becomes

$$\int_{-1}^1 ds F(s) \delta(W_p - W_q) = \frac{F(s_*)}{|W'(p)| |dq/ds|_{s_*}} = \frac{F(s_*)}{k|W'(p)|}, \quad (97)$$

where the ' denotes the derivative with respect to  $p$ . Consequently, the  $(p, s)$  integral reduces to a single  $p$ -integral

$$\int_0^\infty dp p^6 \int_{-1}^1 ds (1-s^2)^2 \frac{n_p(\tau)n_q(\tau)}{W_p(\tau)W_q(\tau)} \cdot \mathcal{T}_{pq}(\tau) \implies \frac{\pi}{k|W'(p)|} \left(1 - \frac{k^2}{4p^2}\right)^2 \frac{n_p^2}{W_p^2}, \quad \text{with } p \geq \frac{k}{2}. \quad (98)$$

Putting everything together by plugging (98) and (82) into (80), we get the final expression for the power spectrum,

$$P_h^{\text{prim}}(k) \simeq \frac{8}{\pi^3 M_{\text{Pl}}^4} \int_{-\infty}^0 d\tau j_1^2(k\tau) \int_{k/2}^{\infty} dp p^6 \frac{1}{|W'(p; \tau)|} \left(1 - \frac{k^2}{4p^2}\right)^2 \frac{n_p^2(\tau)}{W_p^2(\tau)} \quad (99)$$

For the adiabatic frequency where  $W(p, \tau) \simeq \sqrt{p^2 + M_{\text{eff}}^2(\tau)}$ , we have  $W'(p, \tau) = \partial W / \partial p = p/W$ . Finally, the integral simplifies to,

$$P_h^{\text{prim}}(k) \simeq \frac{8}{\pi^3 M_{\text{Pl}}^4} \int_{-\infty}^0 d\tau j_1^2(k\tau) \int_{k/2}^{\infty} dp p^5 \left(1 - \frac{k^2}{4p^2}\right)^2 \frac{n_p^2(\tau)}{W_p(\tau)}. \quad (100)$$

## References

- [1] A. H. Guth, “The Inflationary Universe: A Possible Solution to the Horizon and Flatness Problems,” *Phys. Rev. D* **23** (1981) 347–356.
- [2] A. A. Starobinsky, “Spectrum of relict gravitational radiation and the early state of the universe,” *JETP Lett.* **30** (1979) 682–685.
- [3] A. D. Linde, “A New Inflationary Universe Scenario: A Possible Solution of the Horizon, Flatness, Homogeneity, Isotropy and Primordial Monopole Problems,” *Phys. Lett. B* **108** (1982) 389–393.
- [4] A. Albrecht and P. J. Steinhardt, “Cosmology for Grand Unified Theories with Radiatively Induced Symmetry Breaking,” *Phys. Rev. Lett.* **48** (1982) 1220–1223.
- [5] I. Affleck and M. Dine, “A New Mechanism for Baryogenesis,” *Nucl. Phys. B* **249** (1985) 361–380.
- [6] R. N. Mohapatra and N. Okada, “Affleck-Dine baryogenesis with observable neutron-antineutron oscillation,” *Phys. Rev. D* **104** no. 5, (2021) 055030, [arXiv:2107.01514 \[hep-ph\]](https://arxiv.org/abs/2107.01514).
- [7] M. P. Hertzberg and J. Karouby, “Generating the Observed Baryon Asymmetry from the Inflaton Field,” *Phys. Rev. D* **89** no. 6, (2014) 063523, [arXiv:1309.0010 \[hep-ph\]](https://arxiv.org/abs/1309.0010).
- [8] K. D. Lozanov and M. A. Amin, “End of inflation, oscillons, and matter-antimatter asymmetry,” *Phys. Rev. D* **90** no. 8, (2014) 083528, [arXiv:1408.1811 \[hep-ph\]](https://arxiv.org/abs/1408.1811).
- [9] M. Yamada, “Affleck-Dine baryogenesis just after inflation,” *Phys. Rev. D* **93** no. 8, (2016) 083516, [arXiv:1511.05974 \[hep-ph\]](https://arxiv.org/abs/1511.05974).
- [10] K. Bamba, N. D. Barrie, A. Sugamoto, T. Takeuchi, and K. Yamashita, “Ratchet baryogenesis and an analogy with the forced pendulum,” *Mod. Phys. Lett. A* **33** no. 17, (2018) 1850097, [arXiv:1610.03268 \[hep-ph\]](https://arxiv.org/abs/1610.03268).

- [11] K. Bamba, N. D. Barrie, A. Sugamoto, T. Takeuchi, and K. Yamashita, “Pendulum Leptogenesis,” *Phys. Lett. B* **785** (2018) 184–190, [arXiv:1805.04826 \[hep-ph\]](https://arxiv.org/abs/1805.04826).
- [12] Y.-Y. Charng, D.-S. Lee, C. N. Leung, and K.-W. Ng, “Affleck-Dine Baryogenesis, Split Supersymmetry, and Inflation,” *Phys. Rev. D* **80** (2009) 063519, [arXiv:0802.1328 \[hep-ph\]](https://arxiv.org/abs/0802.1328).
- [13] Y.-P. Wu, L. Yang, and A. Kusenko, “Leptogenesis from spontaneous symmetry breaking during inflation,” *JHEP* **12** (2019) 088, [arXiv:1905.10537 \[hep-ph\]](https://arxiv.org/abs/1905.10537).
- [14] C.-M. Lin and K. Kohri, “Inflaton as the Affleck-Dine Baryogenesis Field in Hilltop Supernatural Inflation,” *Phys. Rev. D* **102** no. 4, (2020) 043511, [arXiv:2003.13963 \[hep-ph\]](https://arxiv.org/abs/2003.13963).
- [15] N. D. Barrie, A. Sugamoto, T. Takeuchi, and K. Yamashita, “Higgs Inflation, Vacuum Stability, and Leptogenesis,” *JHEP* **08** (2020) 072, [arXiv:2001.07032 \[hep-ph\]](https://arxiv.org/abs/2001.07032).
- [16] H. An, Q. Chen, and Y. Yin, “A model for inflaton induced baryogenesis and its phenomenological consequences,” *JHEP* **06** (2025) 222, [arXiv:2409.05833 \[astro-ph.CO\]](https://arxiv.org/abs/2409.05833).
- [17] A. Bodas, S. Kumar, and R. Sundrum, “The Scalar Chemical Potential in Cosmological Collider Physics,” *JHEP* **02** (2021) 079, [arXiv:2010.04727 \[hep-ph\]](https://arxiv.org/abs/2010.04727).
- [18] A. Bodas, E. Broadberry, and R. Sundrum, “Grand unification at the cosmological collider with chemical potential,” *JHEP* **01** (2025) 115, [arXiv:2409.07524 \[hep-ph\]](https://arxiv.org/abs/2409.07524).
- [19] A. Bodas, E. Broadberry, R. Sundrum, and Z. Xu, “Charged Loops at the Cosmological Collider with Chemical Potential,” [arXiv:2507.22978 \[hep-ph\]](https://arxiv.org/abs/2507.22978).
- [20] E. W. Kolb, D. J. H. Chung, and A. Riotto, “WIMPzillas!,” *AIP Conf. Proc.* **484** no. 1, (1999) 91–105, [arXiv:hep-ph/9810361](https://arxiv.org/abs/hep-ph/9810361).
- [21] H. An, X. Tong, and S. Zhou, “Superheavy dark matter production from a symmetry-restoring first-order phase transition during inflation,” *Phys. Rev. D* **107** no. 2, (2023) 023522, [arXiv:2208.14857 \[hep-ph\]](https://arxiv.org/abs/2208.14857).
- [22] L. Li, T. Nakama, C. M. Sou, Y. Wang, and S. Zhou, “Gravitational Production of Superheavy Dark Matter and Associated Cosmological Signatures,” *JHEP* **07** (2019) 067, [arXiv:1903.08842 \[astro-ph.CO\]](https://arxiv.org/abs/1903.08842).
- [23] L. Li, S. Lu, Y. Wang, and S. Zhou, “Cosmological Signatures of Superheavy Dark Matter,” *JHEP* **07** (2020) 231, [arXiv:2002.01131 \[hep-ph\]](https://arxiv.org/abs/2002.01131).
- [24] P. Adshead, L. Pearce, M. Peloso, M. A. Roberts, and L. Sorbo, “Gravitational waves from fermion production during axion inflation,” *JCAP* **10** (2019) 018, [arXiv:1904.10483 \[astro-ph.CO\]](https://arxiv.org/abs/1904.10483).

[25] L. Kofman, A. D. Linde, and A. A. Starobinsky, “Towards the theory of reheating after inflation,” *Phys. Rev. D* **56** (1997) 3258–3295, [arXiv:hep-ph/9704452](https://arxiv.org/abs/hep-ph/9704452).

[26] Y. Ema, R. Jinno, K. Mukaida, and K. Nakayama, “Gravitational Effects on Inflaton Decay,” *JCAP* **05** (2015) 038, [arXiv:1502.02475](https://arxiv.org/abs/1502.02475) [hep-ph].

[27] Y. Ema, R. Jinno, K. Mukaida, and K. Nakayama, “Gravitational particle production in oscillating backgrounds and its cosmological implications,” *Phys. Rev. D* **94** no. 6, (2016) 063517, [arXiv:1604.08898](https://arxiv.org/abs/1604.08898) [hep-ph].

[28] Y. Ema, K. Nakayama, and Y. Tang, “Production of Purely Gravitational Dark Matter,” *JHEP* **09** (2018) 135, [arXiv:1804.07471](https://arxiv.org/abs/1804.07471) [hep-ph].

[29] E. W. Kolb and A. J. Long, “Cosmological gravitational particle production and its implications for cosmological relics,” *Rev. Mod. Phys.* **96** no. 4, (2024) 045005, [arXiv:2312.09042](https://arxiv.org/abs/2312.09042) [astro-ph.CO].

[30] J. L. Cook and L. Sorbo, “Particle production during inflation and gravitational waves detectable by ground-based interferometers,” *Phys. Rev. D* **85** (2012) 023534, [arXiv:1109.0022](https://arxiv.org/abs/1109.0022) [astro-ph.CO]. [Erratum: Phys.Rev.D 86, 069901 (2012)].

[31] **LIGO Scientific, KAGRA, VIRGO** Collaboration, R. Abbott *et al.*, “Search for Gravitational-wave Transients Associated with Magnetar Bursts in Advanced LIGO and Advanced Virgo Data from the Third Observing Run,” *Astrophys. J.* **966** no. 1, (2024) 137, [arXiv:2210.10931](https://arxiv.org/abs/2210.10931) [astro-ph.HE].

[32] **LISA** Collaboration, P. Amaro-Seoane *et al.*, “Laser Interferometer Space Antenna,” [arXiv:1702.00786](https://arxiv.org/abs/1702.00786) [astro-ph.IM].

[33] **TianQin** Collaboration, J. Luo *et al.*, “TianQin: a space-borne gravitational wave detector,” *Class. Quant. Grav.* **33** no. 3, (2016) 035010, [arXiv:1512.02076](https://arxiv.org/abs/1512.02076) [astro-ph.IM].

[34] W.-H. Ruan, Z.-K. Guo, R.-G. Cai, and Y.-Z. Zhang, “Taiji Program: Gravitational-Wave Sources,” *Int. J. Mod. Phys. A* **35** no. 17, (2020) 2050075, [arXiv:1807.09495](https://arxiv.org/abs/1807.09495) [gr-qc].

[35] **NANOGrav** Collaboration, G. Agazie *et al.*, “The NANOGrav 15 yr Data Set: Observations and Timing of 68 Millisecond Pulsars,” *Astrophys. J. Lett.* **951** no. 1, (2023) L9, [arXiv:2306.16217](https://arxiv.org/abs/2306.16217) [astro-ph.HE].

[36] **EPTA** Collaboration, J. Antoniadis *et al.*, “The second data release from the European Pulsar Timing Array - I. The dataset and timing analysis,” *Astron. Astrophys.* **678** (2023) A48, [arXiv:2306.16224](https://arxiv.org/abs/2306.16224) [astro-ph.HE].

[37] A. Zic *et al.*, “The Parkes Pulsar Timing Array third data release,” *Publ. Astron. Soc. Austral.* **40** (2023) e049, [arXiv:2306.16230](https://arxiv.org/abs/2306.16230) [astro-ph.HE].

[38] H. Xu *et al.*, “Searching for the Nano-Hertz Stochastic Gravitational Wave Background with the Chinese Pulsar Timing Array Data Release I,” *Res. Astron. Astrophys.* **23** no. 7, (2023) 075024, [arXiv:2306.16216 \[astro-ph.HE\]](https://arxiv.org/abs/2306.16216).

[39] **NANOGrav** Collaboration, G. Agazie *et al.*, “The NANOGrav 15 yr Data Set: Evidence for a Gravitational-wave Background,” *Astrophys. J. Lett.* **951** no. 1, (2023) L8, [arXiv:2306.16213 \[astro-ph.HE\]](https://arxiv.org/abs/2306.16213).

[40] **EPTA, InPTA:** Collaboration, J. Antoniadis *et al.*, “The second data release from the European Pulsar Timing Array - III. Search for gravitational wave signals,” *Astron. Astrophys.* **678** (2023) A50, [arXiv:2306.16214 \[astro-ph.HE\]](https://arxiv.org/abs/2306.16214).

[41] D. J. Reardon *et al.*, “Search for an Isotropic Gravitational-wave Background with the Parkes Pulsar Timing Array,” *Astrophys. J. Lett.* **951** no. 1, (2023) L6, [arXiv:2306.16215 \[astro-ph.HE\]](https://arxiv.org/abs/2306.16215).

[42] **NANOGrav** Collaboration, M. Vallisneri *et al.*, “Modeling the uncertainties of solar-system ephemerides for robust gravitational-wave searches with pulsar timing arrays,” [arXiv:2001.00595 \[astro-ph.HE\]](https://arxiv.org/abs/2001.00595).

[43] **CMB-S4** Collaboration, K. N. Abazajian *et al.*, *CMB-S4 Science Book, First Edition*. 10, 2016. [arXiv:1610.02743 \[astro-ph.CO\]](https://arxiv.org/abs/1610.02743).

[44] P. Adshead and E. I. Sfakianakis, “Fermion production during and after axion inflation,” *JCAP* **11** (2015) 021, [arXiv:1508.00891 \[hep-ph\]](https://arxiv.org/abs/1508.00891).

[45] L.-T. Wang and Z.-Z. Xianyu, “Gauge Boson Signals at the Cosmological Collider,” *JHEP* **11** (2020) 082, [arXiv:2004.02887 \[hep-ph\]](https://arxiv.org/abs/2004.02887).

[46] X. Tong and Z.-Z. Xianyu, “Large spin-2 signals at the cosmological collider,” *JHEP* **10** (2022) 194, [arXiv:2203.06349 \[hep-ph\]](https://arxiv.org/abs/2203.06349).

[47] Z. Qin and Z.-Z. Xianyu, “Helical inflation correlators: partial Mellin-Barnes and bootstrap equations,” *JHEP* **04** (2023) 059, [arXiv:2208.13790 \[hep-th\]](https://arxiv.org/abs/2208.13790).

[48] C. M. Sou, X. Tong, and Y. Wang, “Chemical-potential-assisted particle production in FRW spacetimes,” *JHEP* **06** (2021) 129, [arXiv:2104.08772 \[hep-th\]](https://arxiv.org/abs/2104.08772).

[49] Y. Yamada, “Superadiabatic basis in cosmological particle production: application to preheating,” *JCAP* **09** (2021) 009, [arXiv:2106.06111 \[hep-th\]](https://arxiv.org/abs/2106.06111).

[50] J. Preskill, “Quantum field theory in curved spacetime.” 1990.

[51] L. Parker and S. A. Fulling, “Adiabatic regularization of the energy momentum tensor of a quantized field in homogeneous spaces,” *Phys. Rev. D* **9** (1974) 341–354.

[52] N. D. Birrell and P. C. W. Davies, *Quantum Fields in Curved Space*. Cambridge Monographs on Mathematical Physics. Cambridge University Press, Cambridge, UK, 1982.

[53] P. R. Anderson and L. Parker, “Adiabatic Regularization in Closed Robertson-walker Universes,” *Phys. Rev. D* **36** (1987) 2963.

[54] B. Allen and J. D. Romano, “Detecting a stochastic background of gravitational radiation: Signal processing strategies and sensitivities,” *Phys. Rev. D* **59** (1999) 102001, [arXiv:gr-qc/9710117](https://arxiv.org/abs/gr-qc/9710117).

[55] S. Weinberg, “Damping of tensor modes in cosmology,” *Phys. Rev. D* **69** (2004) 023503, [arXiv:astro-ph/0306304](https://arxiv.org/abs/astro-ph/0306304).

[56] M. Maggiore, *Gravitational Waves. Vol. 1: Theory and Experiments*. Oxford University Press, 2007.

[57] C. Caprini and D. G. Figueira, “Cosmological Backgrounds of Gravitational Waves,” *Class. Quant. Grav.* **35** no. 16, (2018) 163001, [arXiv:1801.04268](https://arxiv.org/abs/1801.04268) [astro-ph.CO].

[58] S. Kawamura *et al.*, “Current status of space gravitational wave antenna DECIGO and B-DECIGO,” *PTEP* **2021** no. 5, (2021) 05A105, [arXiv:2006.13545](https://arxiv.org/abs/2006.13545) [gr-qc].

[59] ET Collaboration, A. Abac *et al.*, “The Science of the Einstein Telescope,” [arXiv:2503.12263](https://arxiv.org/abs/2503.12263) [gr-qc].

[60] D. Reitze *et al.*, “Cosmic Explorer: The U.S. Contribution to Gravitational-Wave Astronomy beyond LIGO,” *Bull. Am. Astron. Soc.* **51** (7, 2019) 035, [arXiv:1907.04833](https://arxiv.org/abs/1907.04833) [astro-ph.IM].

[61] N. Arkani-Hamed and J. Maldacena, “Cosmological collider physics.” 2015.

[62] X. Chen and Y. Wang, “Quasi-Single Field Inflation and Non-Gaussianities,” *JCAP* **04** (2010) 027, [arXiv:0911.3380](https://arxiv.org/abs/0911.3380) [hep-th].

[63] J. Hubisz, S. J. Lee, H. Li, and B. Sambasivam, “Cosmological quasiparticles and the cosmological collider,” *Phys. Rev. D* **111** no. 2, (2025) 023543, [arXiv:2408.08951](https://arxiv.org/abs/2408.08951) [astro-ph.CO].

[64] H. Lee, D. Baumann, and G. L. Pimentel, “Non-Gaussianity as a Particle Detector,” *JHEP* **12** (2016) 040, [arXiv:1607.03735](https://arxiv.org/abs/1607.03735) [hep-th].

[65] X. Chen, Y. Wang, and Z.-Z. Xianyu, “Schwinger-Keldysh Diagrammatics for Primordial Perturbations,” *JCAP* **12** (2017) 006, [arXiv:1703.10166](https://arxiv.org/abs/1703.10166) [hep-th].

[66] Y. Cui and Z.-Z. Xianyu, “Probing Leptogenesis with the Cosmological Collider,” *Phys. Rev. Lett.* **129** no. 11, (2022) 111301, [arXiv:2112.10793](https://arxiv.org/abs/2112.10793) [hep-ph].

[67] L.-T. Wang and Z.-Z. Xianyu, “In Search of Large Signals at the Cosmological Collider,” *JHEP* **02** (2020) 044, [arXiv:1910.12876](https://arxiv.org/abs/1910.12876) [hep-ph].

[68] L.-T. Wang and Z.-Z. Xianyu, “Gauge Boson Signals at the Cosmological Collider,” *JHEP* **11** (2020) 082, [arXiv:2004.02887](https://arxiv.org/abs/2004.02887) [hep-ph].

[69] X. Chen, Y. Wang, and Z.-Z. Xianyu, “Neutrino Signatures in Primordial Non-Gaussianities,” *JHEP* **09** (2018) 022, [arXiv:1805.02656 \[hep-ph\]](https://arxiv.org/abs/1805.02656).

[70] X. Chen, Y. Wang, and Z.-Z. Xianyu, “Standard Model Mass Spectrum in Inflationary Universe,” *JHEP* **04** (2017) 058, [arXiv:1612.08122 \[hep-th\]](https://arxiv.org/abs/1612.08122).

[71] X. Chen, Y. Wang, and Z.-Z. Xianyu, “Standard Model Background of the Cosmological Collider,” *Phys. Rev. Lett.* **118** no. 26, (2017) 261302, [arXiv:1610.06597 \[hep-th\]](https://arxiv.org/abs/1610.06597).

[72] X. Chen, Y. Wang, and Z.-Z. Xianyu, “Loop Corrections to Standard Model Fields in Inflation,” *JHEP* **08** (2016) 051, [arXiv:1604.07841 \[hep-th\]](https://arxiv.org/abs/1604.07841).

[73] X. Chen, M. H. Namjoo, and Y. Wang, “Quantum Primordial Standard Clocks,” *JCAP* **02** (2016) 013, [arXiv:1509.03930 \[astro-ph.CO\]](https://arxiv.org/abs/1509.03930).

[74] G. L. Pimentel and D.-G. Wang, “Boostless cosmological collider bootstrap,” *JHEP* **10** (2022) 177, [arXiv:2205.00013 \[hep-th\]](https://arxiv.org/abs/2205.00013).

[75] Y. Yin, “Cosmological collider signal from non-Bunch-Davies initial states,” *Phys. Rev. D* **109** no. 4, (2024) 043535, [arXiv:2309.05244 \[hep-ph\]](https://arxiv.org/abs/2309.05244).

[76] S. Aoki and M. Yamaguchi, “Disentangling mass spectra of multiple fields in cosmological collider,” *JHEP* **04** (2021) 127, [arXiv:2012.13667 \[hep-th\]](https://arxiv.org/abs/2012.13667).

[77] L. Pinol, S. Aoki, S. Renaux-Petel, and M. Yamaguchi, “Inflationary flavor oscillations and the cosmic spectroscopy,” *Phys. Rev. D* **107** no. 2, (2023) L021301, [arXiv:2112.05710 \[hep-th\]](https://arxiv.org/abs/2112.05710).

[78] S. Aoki, “Continuous spectrum on cosmological collider,” *JCAP* **04** (2023) 002, [arXiv:2301.07920 \[hep-th\]](https://arxiv.org/abs/2301.07920).

[79] S. Aoki and A. Strumia, “Testing the arrow of time at the cosmo collider,” [arXiv:2510.05204 \[hep-ph\]](https://arxiv.org/abs/2510.05204).

[80] S. Aoki, A. Ghoshal, and A. Strumia, “Cosmological collider non-Gaussianity from multiple scalars and  $R^2$  gravity,” *JHEP* **11** (2024) 009, [arXiv:2408.07069 \[astro-ph.CO\]](https://arxiv.org/abs/2408.07069).

[81] S. P. Martin, “A Supersymmetry primer,” *Adv. Ser. Direct. High Energy Phys.* **18** (1998) 1–98, [arXiv:hep-ph/9709356](https://arxiv.org/abs/hep-ph/9709356).

[82] A. Caravano, E. Komatsu, K. D. Lozanov, and J. Weller, “Lattice simulations of axion-U(1) inflation,” *Phys. Rev. D* **108** no. 4, (2023) 043504, [arXiv:2204.12874 \[astro-ph.CO\]](https://arxiv.org/abs/2204.12874).

[83] A. Berera, “Warm inflation,” *Phys. Rev. Lett.* **75** (1995) 3218–3221, [arXiv:astro-ph/9509049](https://arxiv.org/abs/astro-ph/9509049).

[84] A. Berera, I. G. Moss, and R. O. Ramos, “Warm Inflation and its Microphysical Basis,” *Rept. Prog. Phys.* **72** (2009) 026901, [arXiv:0808.1855 \[hep-ph\]](https://arxiv.org/abs/0808.1855).

- [85] R. Z. Ferreira and A. Notari, “Thermalized Axion Inflation,” *JCAP* **09** (2017) 007, [arXiv:1706.00373 \[astro-ph.CO\]](https://arxiv.org/abs/1706.00373).
- [86] K. V. Berghaus, P. W. Graham, and D. E. Kaplan, “Minimal Warm Inflation,” *JCAP* **03** (2020) 034, [arXiv:1910.07525 \[hep-ph\]](https://arxiv.org/abs/1910.07525). [Erratum: JCAP 10, E02 (2023)].
- [87] K. V. Berghaus, M. Drewes, and S. Zell, “Warm Inflation with the Standard Model,” *Phys. Rev. Lett.* **135** no. 17, (2025) 171002, [arXiv:2503.18829 \[hep-ph\]](https://arxiv.org/abs/2503.18829).